Bi-Sr-Ca-Cu-O THIN FILMS GROWN BY FLASH EVAPORATION AND PULSED LASER DEPOSITION

A Thesis

by

SANTHANA GOPINATH GANAPATHY SUBRAMANIAN

Submitted to the Office of Graduate Studies of
Texas A&M University
in partial fulfillment of the requirements for the degree of

MASTER OF SCIENCE

December 2003

Major Subject: Mechanical Engineering

Bi-Sr-Ca-Cu-O THIN FILMS GROWN BY FLASH EVAPORATION AND PULSED LASER DEPOSITION

A Thesis

by

SANTHANA GOPINATH GANAPATHY SUBRAMANIAN

Submitted to Texas A&M University
in partial fulfillment of the requirements
for the degree of

MASTER OF SCIENCE

Approved as to style and content by:

_____	_____
M. Yavuz (Co-Chair of Committee)	D. G. Naugle (Co-Chair of Committee)
_____	_____
K. T. Hartwig Jr. (Member)	D. L. O'Neal (Head of Department)
_____	
R. J. Morgan (Member)	

December 2003

Major Subject: Mechanical Engineering

ABSTRACT

Bi-Sr-Ca-Cu-O Thin Films Grown by Flash Evaporation and Pulsed Laser Deposition.

(December 2003)

Santhana Gopinath Ganapathy Subramanian, B.E., University of Mysore

Co-Chairs of Advisory Committee: Dr. M. Yavuz
Dr. D.G. Naugle

Bismuth-Strontium-Calcium-Copper-Oxide (BSCCO) compounds are an important family of compounds that have one of the highest transition temperatures among all high-temperature superconductors. The compound is known to exist in three distinct phases, commonly referred to as the 2201, 2212 and 2223 phases. Of these three phases, the 2212 and 2223 phases are the most important, as their transition temperature is higher than the boiling point of liquid nitrogen. It is desirable to produce the compound in thin film form, as the bulk samples are normally polycrystalline.

This thesis compares thin films produced by two techniques for depositing BSCCO in order to understand the effect of various processing parameters on the final quality of the thin films. Thin films were grown by flash evaporation at Texas A&M University, and by pulsed laser deposition (PLD) at the University of Wollongong, Australia. The latter of these techniques is widely used for growing thin films of various compounds. Single-phase 2212 films were grown on a MgO substrate using the pulsed laser deposition technique from commercially available 2212 powder. The effect of annealing on the thin films was also studied.

ACKNOWLEDGEMENTS

I would like to express my gratitude to my advisor, Dr. Mustafa Yavuz, for his support, patience, and encouragement throughout my graduate studies. It is not often that one finds an advisor and colleague who always finds the time for listening to the little problems and roadblocks that unavoidably crop up in the course of performing research. His technical and editorial advice was essential to the completion of this thesis and he has taught me innumerable lessons and insights into the workings of academic research in general.

My thanks also go to the members of my committee, Dr. Ted Hartwig, Dr. Donald Naugle and Dr. Roger Morgan for reading previous drafts and providing many valuable comments that improved the presentation and contents of this thesis.

TABLE OF CONTENTS

LIST OF FIGURES

LIST OF TABLES

CHAPTER I
INTRODUCTION

A high critical temperature is one of the most important qualities that is desired of modern day superconductors. Materials that have a T_C above the boiling point of liquid nitrogen have been successfully manufactured by many previous researchers. This results in a huge saving in the cost of operation, as liquid nitrogen is inexpensive and more abundantly available when compared to liquid helium. The earth's atmosphere is itself made up of more than 70% of nitrogen. These superconductors are commonly referred to as high temperature superconductors (HTS). Among this class of superconductors, of particular interest is the compound commonly referred to as BSCCO. It was discovered in 1988 by Hiroshi Maeda and others [1]. It is desirable to grow these compounds in thin film form for a variety of reasons that will be described later in this document. Among the other desirable qualities are the singularity of phase and crystallinity of the film.

Much effort has been directed towards growing the films in single crystal thin film form by a variety of methods. It is also highly desirable that the as-deposited thin films have the required properties. Post-deposition annealing methods are normally useful in enhancing the properties of the film, but these processes also promote diffusion. If the thin films are to be employed in a circuit, it is unadvisable to anneal them after the circuit has been patterned over them. A variety of methods have been employed with varying degrees of success in order to fabricate thin films of BSCCO. Among these are Molecular Beam Epitaxy, Sputtering, Pulsed Laser Deposition and Flash Evaporation.

This thesis follows the style and format of the Journal of Crystal Growth.

The focus of this work is to compare the properties of thin BSCCO films grown by flash evaporation and pulsed laser deposition (PLD). A series of BSCCO thin films prepared by PLD by the Institute for Superconducting and Electronic Materials (ISEM) at the University of Wollongong, Australia have been characterized by the author and compared with those grown by flash evaporation and characterized at Texas A&M University by the author. The X-ray diffraction analysis of some of the samples was carried out at Lamar University, Beaumont, Texas. Chapter II provides a brief introduction to superconductors in general and also to bismuth based superconductors. Chapter III describes the powder processing, also known as bulk preparation, of BSCCO. Chapters IV and V present earlier work done using flash evaporation and pulsed laser deposition respectively, and also the results obtained in this study. Chapter VI provides a description of other techniques that have been successfully employed to grow thin films of BSCCO, namely sputtering and molecular beam epitaxy. The appendix provides a description of the characterization techniques employed.

CHAPTER II
INTRODUCTION TO SUPERCONDUCTIVITY

A. HISTORY OF SUPERCONDUCTORS

The discovery of high temperature superconductors has evoked new interest in superconductivity, which was but a mere scientific curiosity before their advent. This discovery has been described as the most significant development since that of the solid state transistor. This explains the unprecedented research effort that is currently being devoted to find new applications for this phenomenon, while trying to develop a better understanding of the same. To appreciate the magnitude of this discovery, it is necessary to look at the history of superconductivity.

Major advances in low-temperature refrigeration were made during the late nineteenth century. The Dutch physicist, Heike Kammerlingh Onnes, first discovered superconductivity in 1911. In 1908, he successfully liquefied helium by cooling it to 4 K. In 1911, he started exploring the electrical properties of metals at extremely low temperatures. Some scientists, such as Lord Kelvin believed that as the temperature of a conductor is lowered, it would level off at a certain ill-defined temperature, allowing the current to flow with little or no resistance. To see what actually happens, Onnes passed a current through a wire of pure mercury at low temperature. Mercury was chosen because it could be obtained in a very pure form. There was no leveling off of the resistance, as was expected, but at 4.2 K, the resistance of the mercury wire suddenly vanished. Figure 1 shows the plot that was published demonstrating superconductivity for the first time.

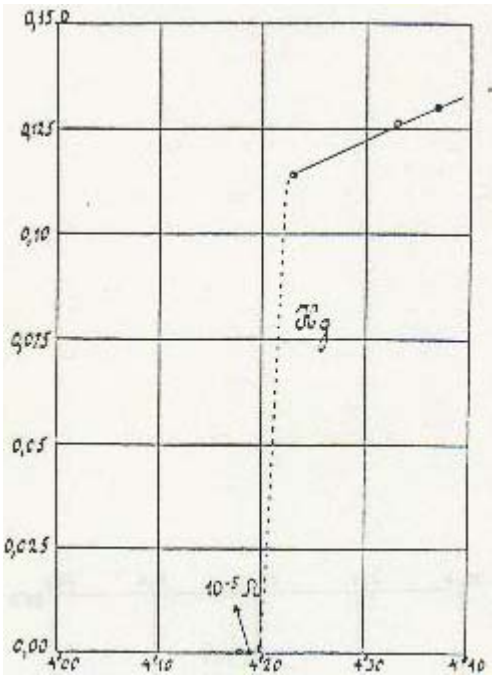

Figure 1. Original plot published by Kammerlingh Onnes marking the discovery of superconductivity in mercury [2]

Since this initial discovery, the DC electrical resistivity of many metals and alloys has also been found to drop to zero within experimental limits when the specimen is cooled to a sufficiently low temperature. This phenomenon is known to exist in many metals and alloys beside mercury [3]. Over the decades, the record T_c slowly increased as researchers explored different materials systems like alloys. In 1973, Nb_3Ge was found to display a T_c of 23.2 K.

Other materials were found to exhibit the property of superconductivity, namely $LiTi_2O_4$ and $BaPb_{1-x}Bi_xO_3$. Although their T_c was of the order of 13 K, they pointed to the fact that superconductivity was not unique to metals and alloys. Bednorz and Müller [4] began exploring a class of compounds composed of lanthanum, barium, copper and oxygen, commonly known as La-Ba-Cu-O. Chu et al. [5] showed that the T_c could be raised by raising the pressure. In 1987, Wang et al. [6] found superconductivity at 90 K in a compound containing yttrium, barium, copper and oxygen. This was significant since this was the first time that a superconductor had broken the liquid nitrogen barrier, since it had a T_c greater than 77.2 K, the boiling point of liquid nitrogen. This meant that the expense of using liquid helium could be avoided by using liquid nitrogen instead, and hence making superconductor applications more viable. These compounds came to be known as high-temperature superconductors (HTS).

An entire series of HTS materials have been found to exist when almost any rare earth atom is substituted for yttrium. In 1988, Maeda et al. [1] announced the discovery of a compound containing bismuth, strontium, calcium, copper and oxygen having a T_c of 110 K, which showed multiple superconducting phases.

B. APPLICATIONS OF SUPERCONDUCTORS

There are many applications of superconductivity. The most commonly mentioned ones are power transmission with extremely low losses, magnetic

levitation and shielding owing to the Meissner effect and high field magnets. Small-scale applications include extremely fast micro electronic switching devices, ultra sensitive detectors, low loss chip interconnects, and for data storage. These areas of application will be briefly discussed.

Great enthusiasm has been generated in using superconductors for power transmission, owing to the extremely low losses in superconductors. Onnes discovered [2] that a current kept circulating for over a year in a loop of lead maintained in its superconducting state. Superconductors could also be used in transformers, and reduce power losses by as 15% or more. Energy storage is also an application, as the current in a closed superconducting loop does not decay.

Superconductors can also be used in motors and generators, thereby reducing their size and weight, and enhancing their efficiency. The ability of superconductors to completely exclude a magnetic field can be used to levitate a mass, for example a train, and hence reduce the losses due to friction.

Magnetic resonance imaging (MRI) is the most widely used application of superconductivity, and is used in medical facilities to generate images of the human body by exposing it to a high magnetic field and is helpful as a non-invasive diagnostic tool. The role of the superconductor is to provide the means to cheaply generate the required high magnetic field.

The Josephson junction, named after Brian Josephson who first predicted the effect, is the fastest switching device that is known. When two

superconductors are separated by a thin insulating layer, a current can flow through the insulator in the absence of any applied potential, owing to the quantum tunneling effect. If, however, the critical Josephson current is exceeded, a finite voltage must be applied across the junction in order to pass current. In superconductors, a small magnetic field can cause significant changes in the current. This effect can be used to bring the junction from zero to finite voltage, two states that can correspond to two logical states denoted by 0 and 1. These changes occur in picoseconds. The switching also occurs with very low power dissipation, which can be used to make high-density circuits with minimum heat dissipation. Figure 2 shows the V-I characteristics of a Josephson junction. The Josephson junction has also been used to build the most sensitive magnetic field detectors, high-frequency mixers and amplifiers known.

In all of these applications, it has been tacitly assumed that the superconductors can carry high enough current density for the above applications. In fact, there is a certain current density, called the critical current density (J_c), which is a characteristic of superconductors. If the current density passing through the superconductor exceeds the critical current density, the sample ceases to be superconducting. This parameter limits the applications of superconductors. Upon the application of small magnetic fields, the J_c is further reduced. Furthermore, for realistic applications, it is necessary to operate at temperatures far below the T_c value of the sample.

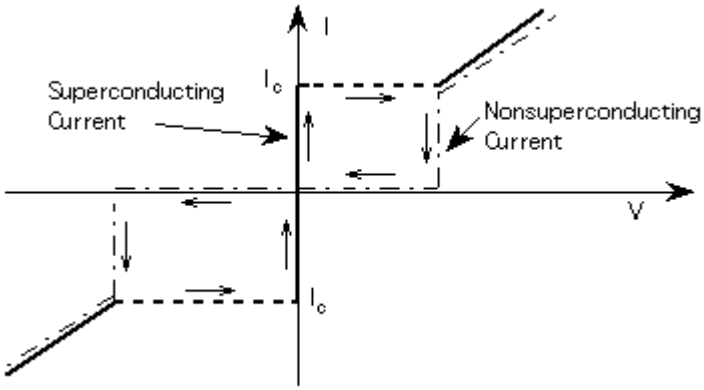

Figure 2. The V-I characteristics of a Josephson junction

C. PRINCIPLES OF SUPERCONDUCTIVITY

The first microscopic theory of superconductors was expounded by Bardeen, Cooper and Schrieffer in 1957 [7]. In the standard BCS model, as an electron moves through a lattice, the lattice itself is distorted, creating a region of high positive charge. This results in the attraction of another electron. Since lattice vibrations are quantified as phonons, this is called the electron-phonon interaction. The second electron that is attracted by the lattice is highly correlated with the first electron, and such a pair is called a Cooper pair. Cooper pairs are continually formed and broken in the lattice at normal temperatures. As the temperature is reduced, the lattice vibration decreases, hence keeping the Cooper pairs intact.

From detailed calculations based on this mechanism, Bardeen, Cooper and Schrieffer were able to develop a formula that relates the superconducting critical temperature to other material properties.

$$T_C = T_D \exp (-1 / NV) \qquad (1)$$

Were T_D is the Debye temperature, which characterizes the lattice vibrational energies, N is the density of electronic states at the Fermi level, and V is a measure of the strength of the attractive electron-electron interaction. For typical materials, T_D is about 300K, which leads to a T_C of about 1-10 K. However, the BCS theory does not account for the existence of HTS materials. The maximum Tc predicted is about 30-40 K. It is still debated as to what causes the phenomenon of superconductivity in the high Tc range.

Perfect conductivity and superconductivity are two different concepts. The distinction was first discovered in 1933 by Meissner and Ochsenfeld [8]. If a perfect conductor is exposed to an increasing magnetic field, currents will be induced to maintain constant flux within the body of the conductor. If the field is

increased from zero, the final induction inside the material will be zero as it was initially. However, if a material is cooled to the perfectly conducting state while in a field, the final induction will be identical to the non-zero starting value. Hence, the final state of the sample depends on its history. In case of ideal superconductors, what Meissner and Ochsenfeld [8] discovered is that the magnetic induction is always zero, no matter what the processing history is. For example, when a superconductor is cooled in an external magnetic field, shielding currents will arise to spontaneously expel the magnetic flux within. This spontaneous expulsion of any magnetic field within the superconductor is referred to as the Meissner effect. If the external magnetic field is raised above some critical value H_C, the material loses its superconductivity. With respect to the H_C, there are two types of superconductors, referred to as Type I and Type II superconductors.

A Type I superconductor at a temperature below its T_C exhibits perfect diamagnetism and excludes a magnetic field up to some critical field H_C, beyond which it reverts back to the normal state, as shown in figure 3A. The magnetization vs. applied external field of a Type II superconductor is shown in figure 3B. When the applied magnetic field is at the critical value H_C, an infinitesimal increase in the applied field will return a Type I superconductor to its normal state.

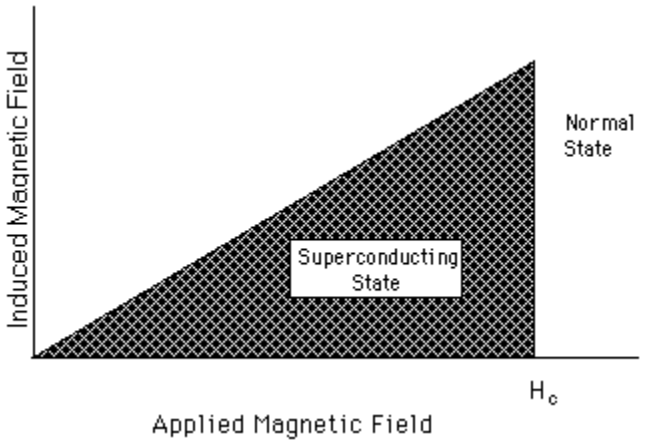

(A)

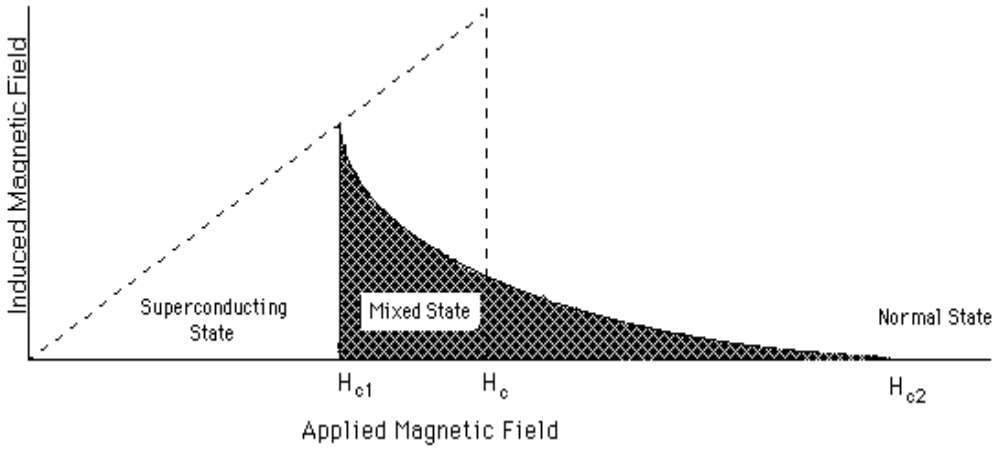

(B)

Figure 3. Induced magnetic field vs. applied magnetic field of: (A) Type I superconductor, (B) Type II superconductor

A Type II superconductor however, is perfectly diamagnetic at fields below H_{C1} and displays similar properties as a Type I superconductor. Upon increasing the field strength to a value larger than H_{C1}, the material will not revert to its normal state on increasing the applied magnetic field beyond the critical value. The field penetrates the interior of the material and the superconductor is said to be in a mixed state. At fields above H_{c2}, the normal state exists.

When in this mixed state, the penetration of the field into the body of the superconductor forms an interesting pattern. The Russian physicist Alexei A. Abrikosov predicted the existence of Type II superconductors as a particular solution of the Ginzburg-Landau equations [9]. His work predicted that in the mixed state, there would be periodic arrays of non-superconducting regimes surrounded by superconducting regions. These non-superconducting regimes allow the magnetic field to completely pass through, and part of this field leaks out into the superconducting region. In figure 4, the solid black line indicates the strength of the magnetic field in the body of the superconductor. It is highest at the core of the vortex, where the field penetrates completely. If the magnitude of the applied field is increased, the diameter of the vortex core remains the same, but the number of vortices increases, and at H_{C2}, the vortex cores overlap, and the material reverts to its normal state.

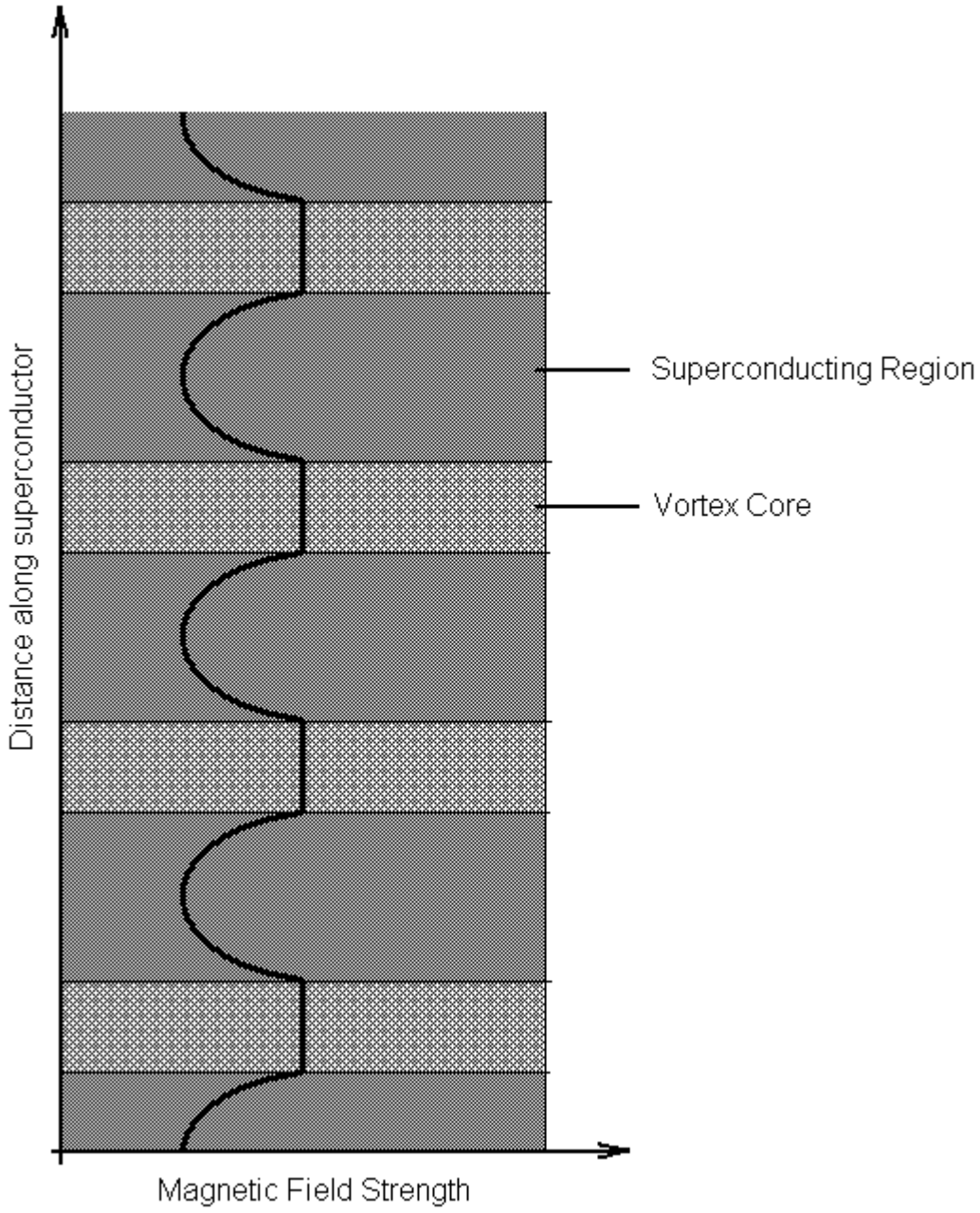

Figure 4. Magnetic field penetration in a Type II superconductor

D. BISMUTH BASED SUPERCONDUCTORS

Bismuth based superconductors were discovered later than the family of yttrium based superconductors, and have distinct advantages over them. The main advantages are higher transition temperatures, higher critical currents, resistance to attack by water, the absence of rare earth elements, the easy availability and high purity of the elements that make up the superconductor, and the applicability of standard crystal growing techniques to their synthesis. Though they have all these advantages, optimizing the growth parameters is still a difficult task, and has not yet been achieved.

These superconductors have a crystal structure commonly known as the modified perovskite structure. The family of perovskite materials has the generic formula ABO_3. The designation “perovskite” originates from the mineral $CaTiO_3$, and the technological interest in this family of materials stems from the discovery of strong ferroelectricity in $BaTiO_3$. It was generally believed that these materials were not metallic. It has been reported that the bismuth-copper oxide superconductors are similar in structure to the bismuth titanate family of ferroelectrics [10]. These materials are found to consist of alternating bismuth oxide and perovskite layers. The general chemical formula of these ferroelectrics is $Bi_2X_{n-1}Y_nO_{3n+3}$, where X=Na, K, Sr, Ca, Ba, Pb and rare earths, Y=Fe, Ga, Cr, Ti, Nb, Ta, W, Cu, and n=1-6. The bismuth-based superconductors (commonly referred to as BSCCO) are among a relatively small number of perovskites that are good conductors. This behavior is due to the fact that some electrons are not localized due to an unusual interaction between copper and oxygen. In materials such as Cu_2O, two copper atoms for an ionic bond with one oxygen atom, and hence, such materials are not conductors.

For oxides such as CuO, however, copper does not give up a second electron as easily as the first, because the loss of a second electron creates a vacancy in the outer shell. It turns out that a filled outer oxygen orbital is slightly

more stable than a filled copper outer orbital, and hence, there is a hole in the outer shell of the copper atoms. Extending this line of reasoning, if copper oxide is alloyed with other elements or compounds, the energy balance can be shifted to a point where both configurations are equally stable, resulting in the sharing of an electron by copper and oxygen. This sharing creates a covalent bond between the two elements, and hence the new material can be a good conductor. While this reasoning is an oversimplification, it explains, albeit qualitatively, how the bismuth copper oxides can be conductors.

It has been well established that there are three distinct phases of BSCCO superconductors. They are commonly referred to as the 2201, 2212 and 2223 phases, having a T_C of 10 K, 80 K and 110 K, respectively. The chemical formula of each of these phases is is $Bi_2Sr_2CuO_x$, $Bi_2Sr_2CaCu_2O_x$ and $Bi_2Sr_2Ca_2Cu_3O_x$, respectively. The ideal crystal structure of each of these phases is shown in figure 5.

The structure of these compounds consists of alternating stacking arrangement of Bi_2O_2 layers and perovskite-like layers along the c-axis. Each Bi_2O_2 layer is composed of two BiO planes with a rock salt like arrangement of Bi and O atoms. Of particular interest is the 2212 phase, as it is thermodynamically more stable, even though it has a lower T_C. The layer sequence of the 2212 phase (sometimes referred to as the 80 K phase) may be described as ……. -CuO_2 – SrO – BiO – BiO – SrO – CuO_2 – Ca – CuO_2 – SrO – BiO – BiO – SrO – CuO_2 ……. The unit cell of such a structure is tetragonal with a=3.8 and c=30.8 angstroms. The ideal structure of the 2223 phase is obtained by inserting a pair of Ca and CuO_2 planes and the 2201 phase is derived by deleting a pair of Ca and CuO_2 layers from the above sequence. The c-axis constants of these two compounds are 37 and 24 Å, respectively.

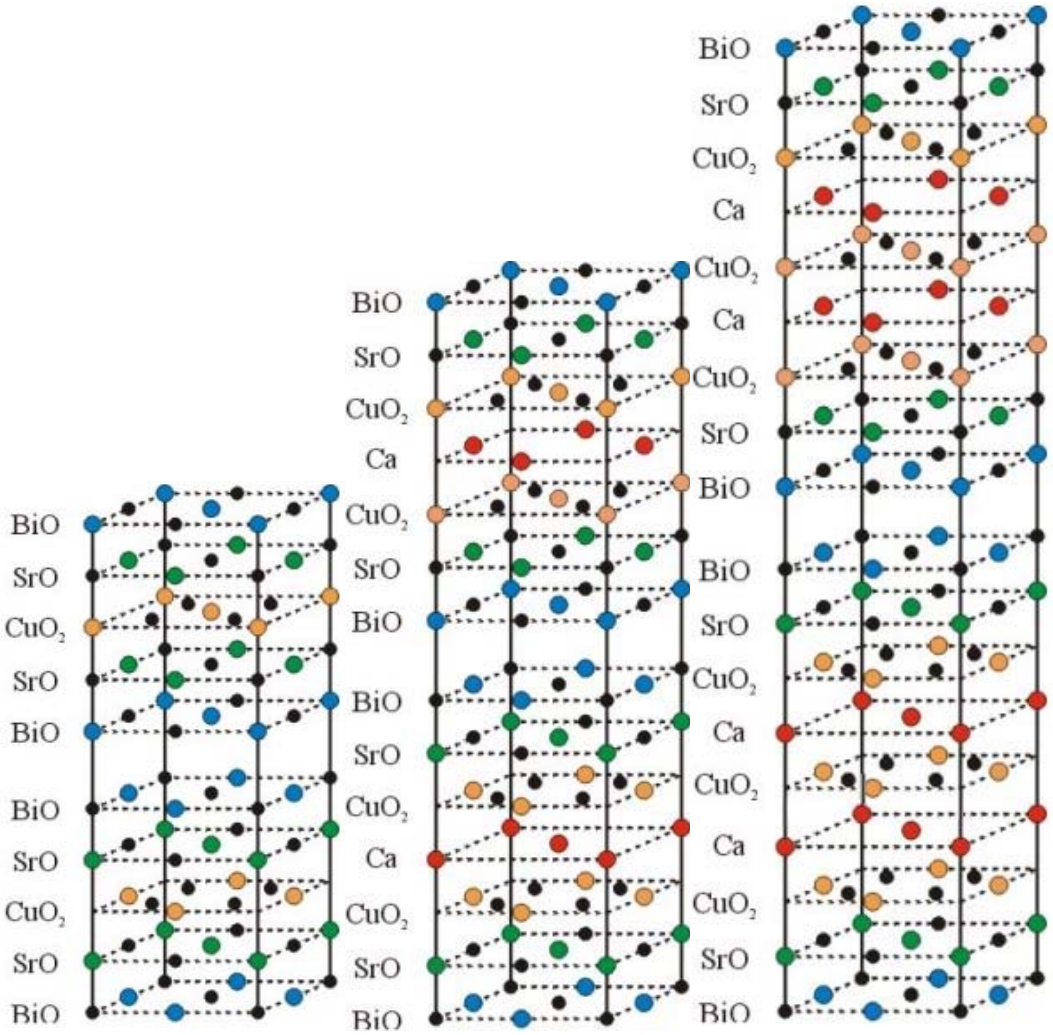

Figure 5. The ideal crystal structure of various BSCCO phases (A) 2201, (B) 2212 (C) 2223

E. THIN FILM SUPERCONDUCTORS

The growth of various elements and compounds in the thin film form has been desirable for a variety of purposes, the main purpose being that compounds can be made very isotropic in the thin film form. This is because thin films, when grown with a particular axis perpendicular to the substrate are two-dimensional. Since the discovery of high T_C superconductors, the field has developed, especially in the commercial sector, with many applications entering the market. Major advances have been made in the production and characteristics of superconducting quantum interference devices (SQUIDs), magnetometry and microwave filters. In the field of logical circuits, superconductors have unique attributes that bring important benefits to digital components. Such circuits operate at picosecond delays and have extremely low power losses. Very low surface resistance at radio and microwave frequencies produces low-loss and low-dispersion transmission lines. The cryogenic temperature of operation virtually eliminates thermal degradation. In the microwave sector, the superconductors suffer losses better than two orders of magnitude less than normal conductors at frequencies of 10 GHz and below. When used as microwave filters, they have a relatively large quality factor Q, which is the ratio between stored energy and dissipated energy.

A principal use of thin film superconductors is in the form of detectors. These detectors for radiation or particles play an important role in many fields of experimental science. Ideally, one would like to measure quantities such as energy of a particle or the wavelength of radiation precisely, but in practice, detectors exhibit only finite resolving power or suffer from other limitations, causing errors to be introduced. Accurate detectors are of prime importance in the field of astrophysics and particle physics. The principle of operation of superconductor based detectors is based on properties that occur only at very low temperatures. The motivation for such detectors is quite compelling.

Bolometers, designed to detect incident power, are popular instruments in space radiometry, for sub-nanometer wavelength observation and thermal imaging for military and biomedical applications. The primary motivation for superconducting detectors was the low resolving power of conventional detection devices. Both semiconducting and superconducting detectors employ the same principle for detection.

Research has been concentrated in order to grow the Type II BSCCO superconductors, especially the 2212 and 2223 phases in the thin film form, in such a way that the c-axis is oriented in a direction perpendicular to the intended direction of current flow. Further, the transport properties are greatly improved if the superconductors have the maximum T_C and are composed, as far as possible, of a single phase. This thesis is an effort to elucidate the role of various deposition methods, deposition conditions and post-deposition processing on the singularity of the phases and improvement of T_C.

CHAPTER III
POWDER PROCESSING

A. BACKGROUND

In order to produce films by any of the methods that are normally used, with the exception of molecular beam epitaxy, preparation of the bulk superconductor is a prerequisite. Ceramic processing of the BSCCO family of materials has been largely investigated by many researchers, with the aim of determining the effect of the processing parameters on the final composition and phase of the bulk samples. The conventional preparation of the bulk involves mixing together the oxides, carbonates or nitrates of the constituent elements and heating them to a high enough temperature so as to initiate the solid state reaction. The mixing may be done by directly mixing the dry powders or by forming a slurry of the powders with an acid. The latter method ensures a more homogeneous powder composition. The phase transition of 2212 to 2223 is described by the following chemical equation

$$Bi_2CaSr_2Cu_2O_8 + 0.5\ Ca_2CuO_3 + 0.5\ CuO \rightarrow Bi_2Ca_2Sr_2Cu_3O_{10}$$

Although this reaction occurs at a wide range of temperatures (850 – 890^{o}C), the most efficient production of the 2223 phase occurs only in the range of 875-890^{o}C. Furthermore, this reaction takes a long time to complete.

It has been found that the BSCCO family of superconductors is highly sensitive to the processing parameters and is rarely found in a single phase. Electron microscopy data has shown that the 2223 phase always occurs with the presence of various other phases, including the 2201 and 2212 phases, oxides of Ca, Sr and Cu, non superconducting Bi-Sr-cuprates and alkaline earth cuprates. Sintered samples are always multiphase with the 2212 phase being

present in greater amounts than the 2223 phase, irrespective of the starting composition or the heating cycle. For example, the sintering of a 2223 stoichiometric powder at 850^{o}C yielded only the 2212 phase. The 2223 phase was observed only after sintering for several days. It is also seen that the formation of the 2223 phase is favored by the formation of a melt at elevated temperatures and extended heating. It is also been shown that the addition of PbO to the starting mixture, usually replacing some of the Bi composition dramatically enhances the formation of the 2223 phase. There have been several theories put forward to explain the formation mechanisms of the 2223 phase, but the exact mechanism is not yet known. Yavuz et al. [11] have experimentally determined that the addition of Pb enhances the formation of the 2223 phase. They employed the use of nitrates as the precursor powders. The nitrates were mixed together in water and the water was evaporated. The resulting powder was calcined at 770^{o}C for 15 hours in air and hand ground using a mortar and pestle and then pressed into the form of a pellet and sintered in air for various periods of time. It was found that the optimum time of sintering is 60 hours, which produces a pellet containing 91% of the 2223 phase, after which the percentage of the 2223 phase rapidly decreases. It is thought that lead doping provides two mechanisms for stabilizing the 2223 phase. The first mechanism is a substitution for bismuth, wherein the lead atom replaces the bismuth sites that are deficient in the number of oxygen atoms surrounding it. Since the Pb ion has a valency of +2, as opposed to +3 for bismuth, it readily assumes the oxygen deficient site. With the valence charges properly compensated, the building blocks of the 2223 structure are stabilized, hence allowing the formation of the phase in abundance. A second mechanism is the liquid phase formation caused by the low melting temperature of lead oxide. It acts as a powerful solvent in the liquid phase, and when the pressed pellet is sintered, it aids the diffusion process of getting atoms to their proper lattice sites for phase formation.

The effects of lead doping can be made more pronounced if the solid state reaction is carried out under low oxygen pressure. This creates more opportunities for lead substitution into oxygen deficient sites simply because there is less oxygen to be incorporated. The melting temperature of PbO is also lowered at low oxygen pressures, thus enhancing the diffusion mechanism. Koyama et al. [12] have reported the formation of an almost single phase 2223 formed in atmospheres of 1/13 O_2 + 12/13 Ar for an optimized starting composition of $Bi_{1.84}Pb_{0.34}Sr_{1.91}Ca_{2.03}Cu_{3.06}O_x$.

B. BULK PREPARATION AND ANALYSIS

The procedure that was finally adopted to prepare the bulk sample involved the following steps. The nitrates of the constituent elements were chosen to be the precursor powders, as they are available commercially at a higher degree of purity as compared to the oxides or carbonates. The amounts of the respective nitrates were taken according to Table 1. These nitrates were added to a mixture of 150 ml of nitric acid and 350 ml of water taken in a beaker, and the beaker was placed on a magnetic stirrer. The setup was started, and the beaker was simultaneously heated to a temperature of 60^{o}C and this was continued until all the liquid had evaporated. The blue-green powder thus obtained was taken in a crucible made of yttrium stabilized zirconia (YSZ) and heated in a furnace to convert the nitrates to oxides. The powder was first heated to 300^{o}C for one hour and then allowed to cool. It was then hand-ground using a mortar and pestle for 30 minutes. It was then calcined at 600^{o}C for 10 hours, allowed to cool, and hand-ground again for 30 minutes. The calcination process was carried out one more time at 700^{o}C for 10 hours. The resulting powder was allowed to cool down, hand ground again, and pressed into the form of a pellet using a pressure of 1.12 x 10^5 psi.

Table 1. Weights of nitrates taken for the preparation of powder used in flash evaporation

Chemical formula	Molecular weight	Weight taken (grams)
$Bi\ (NO_3)_2.5H_2O$	423.066	37.728
$Sr\ (NO_3)_2$	211.633	18.518
$Ca\ (NO_3)_2.4H_2O$	236.153	11.480
$Cu\ (NO_3)_2.2.5H_2O$	232.598	22.614
$Pb\ (NO_3)_2$	331.124	9.966

The resulting pellet was sintered at 800^{o}C for 20 hours, and then quenched in air. It was then broken down into the form of small particles about 2mm across. The theoretical composition of the powder obtained was $Bi_2Sr_{1.96}Ca_{1.09}Cu_{2.18}Pb_{0.15}O_x$. This powder was used for flash evaporation deposition of the films.

The powder prepared above was then characterized by X-ray diffraction. The analysis was carried out at Lamar University, Beaumont on a Bruker S-4 system. The radiation used for the analysis was Cu K-α radiation having a wavelength of 1.54 Å. Instead of employing the conventional point detector, the system has an area detector. The advantage of using an area detector over a point detector is that with both the sample and the detector held stationary, the X-rays diffracting off the sample over a range of angles can be detected. Results of the X-ray diffraction are shown in figure 6. The diffractogram obtained was compared with the results of X-ray diffraction carried out by other groups, namely Kula et al. [13], Wild et al. [14] and Karimoto et al. [15] on films of similar composition, all of whom had used Cu K-α radiation. It is seen that the powder is composed of a mixture of all three phases of BSCCO, and multiple extraneous phases. On comparing with results obtained by Yavuz et al. [16], these phases were also identified to be Ca_2CuO_3 and CuO.

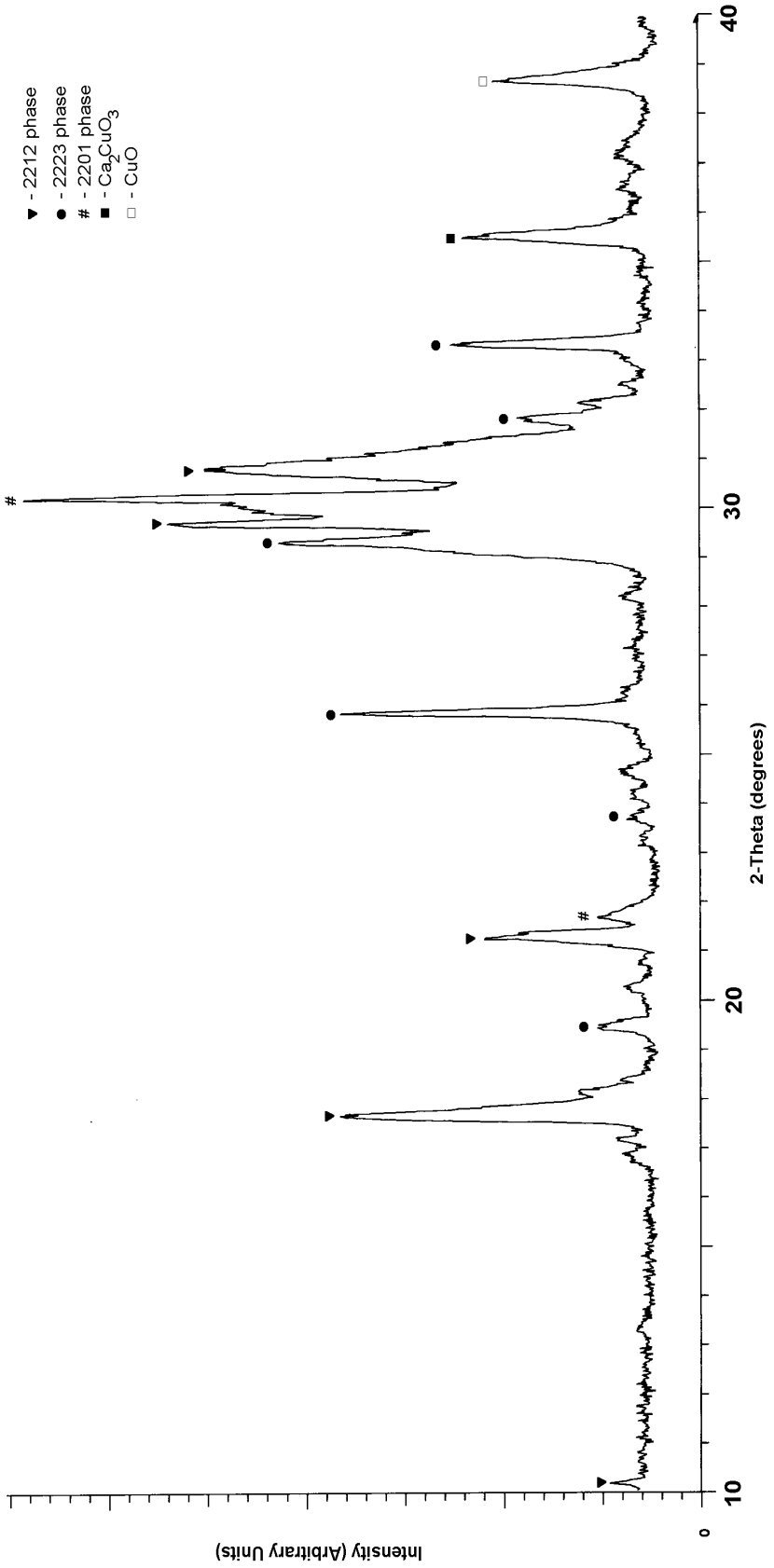

Figure 6. X-ray diffraction pattern of the powder used in flash evaporation

CHAPTER IV
FLASH EVAPORATION

A. BACKGROUND

Among physical vapor deposition techniques thermal evaporation is the one with the longest standing tradition. However, during the last 30 years of booming semiconductor industry which involves a extensive use of thin film technology, deposition techniques like CVD (chemical vapor deposition) or sputtering which often offer unquestionable advantages have been developed to perfection and thermal evaporation has largely been replaced in production lines. On the laboratory scale, due to their simplicity, techniques like pulsed laser deposition or sputtering were much more promising to realize fast results. Consequently, when the new superconductors emerged only a handful of research groups like Berberich [17], Terashima [18], Kwo [19], and Prakash [20] performed deposition trials based on thermal evaporation. The term “thermal evaporation” encompasses both the simple flash evaporation technique and the more complicated and expensive molecular beam epitaxy technique. In this chapter, the flash evaporation technique will be discussed. A schematic of the flash evaporation system used in this study is shown in figure 7. The compound required to be deposited is evaporated in high vacuum. Usually, the chamber is pumped to 10^{-5} torr pressure. During deposition, the distance between the source and the substrate, which is in the range of several tens of centimeters sets the scale for the required mean free path.

The resistively heated boat is probably the simplest of all evaporation sources. Among other evaporation sources are Knudsen cells and electron beam evaporation sources. The latter of these evaporation sources have certain disadvantages when compared to the boat. The Knudsen cell or effusion cell can be used to obtain a metal flux, but not an oxide flux. This would require the

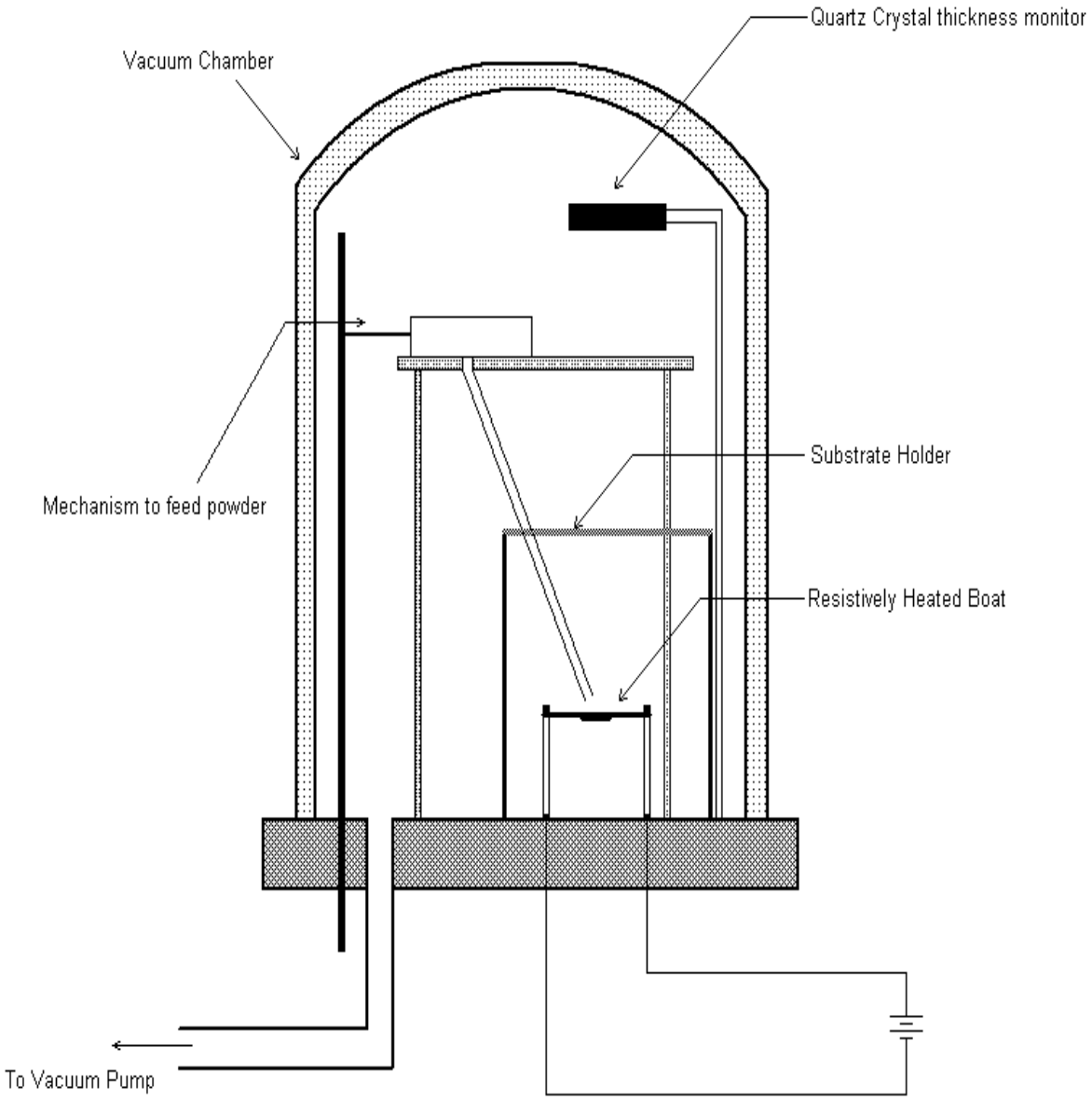

Figure 7. Schematic of flash evaporation system

presence of a reactive gas within the deposition chamber to oxidize the metal flux. This setup would further necessitate the use of high-speed pumps in order to maintain the high vacuum. The Knudsen cells can be used to evaporate single elements only. In order to deposit a multi-component film, a number of cells equal to the number of components present must be employed. Further, the vapor flow rate out of a Knudsen cell is extremely low, about an order of magnitude lower than that of the other sources. Oxide formation would further reduce the flow rate, and in the extreme case, turn off the metal flux completely. As a consequence, these cells will require an online rate monitoring system which has to be very sensitive. To make things even worse the oxide growth of rare earth elements is not a self limiting process but the oxide thickens until the cell eventually fails. For this reason Knudsen cells have been mainly used, for example, by Bozovic et al. [21] and Eckstein et al. [22,23] in MBE type deposition systems with extremely low pressure in connection with activated oxygen confined at the substrate location. Moreover, large capacity Knudsen cells are bulky which limits the uniformity of the film composition across a given area.

Some of these complications can be overcome by electron guns as used, for example, by Naito [24] or Chew et al. [25]. However, due to their short time constants they also put higher requirements to the speed of the rate control. Multi-component film material cannot be evaporated from a single source since most compounds are cracked by the electron beam and will not evaporate stoichiometrically. As a consequence, co-evaporation requires several independent sources. However, electron guns are quite bulky and cannot be positioned as close to each other as would be desirable for realizing a quasi-point source. Only a large source to substrate distance can compensate for this disadvantage, which in turn reduces the material efficiency. In this respect, electron guns and Knudsen cells encounter similar problems.

The resistively heated boat is the simplest of the three evaporation sources considered, but also promises to be the most effective. If the compound to be deposited in thin film form is fed very slowly, with a high enough boat temperature, evaporation of the all the flux arriving at the boat can be assured. This eliminates the problem encountered in the electron beam source, namely that of selective evaporation. However, the boats are quite small and the thickness of the film that can be deposited in one run is quite limited. Another disadvantage of using the boats is the material of the boat. The temperatures that might be required to evaporate a particular compound may be so high as to cause the boat material itself to evaporate and become part of the thin film, which is not at all desirable. In this study, the evaporation source chosen was the resistively heated boat, owing to its simplicity.

The quality of the film is influenced to a great degree by the substrate. For the film to have minimal strain in its lattice, the lattice parameter of the substrate must match that of the film as closely as possible. Sato et al. [26] have reported on the effect of the substrate on the qualities of the film. The lattice mismatch is calculated using the formula

$$\text{Mismatch} = 2(a_s - a_f)/(a_s + a_f)$$

where a_s = lattice parameter of substrate

a_f = lattice parameter of film

The lattice parameter of BSCCO has been calculated by Karimoto et al. [27] to be 3.815 Å. Table 2 shows the lattice parameters of various possible substrates, along with the mismatch of the substrate with BSCCO. Also, SEM images of films deposited by Karimoto et al. show that the number and size of the precipitates present on the surface of the film increases with an increase in the lattice mismatch. Furthermore, Marino et al. [28] have reported an increase in J_C with a decrease in lattice mismatch.

Table 2. Lattice parameter and mismatch of various substrates

Substrate	Lattice parameter (Å)	Mismatch (%)
(0001) Al_2O_3	4.770	+22.25
(100) MgO	4.213	+9.91
(100) SrTiO3	3.904	+2.30
(001) NdGaO3	3.861	+1.20
(001) LaSrGaO4	3.843	+0.47
(001) LaAlO3	3.788	-0.71
(001) YalO3	3.713	-2.71

B. FLASH EVAPORATION OF BSCCO

The system used for flash evaporation was a simple bell-jar arrangement as the deposition chamber. The bell jar could be raised or lowered pneumatically. Fixtures to hold the substrate and a feeding arrangement to feed the powder onto the resistively heated boat were also present. The boat was made of tungsten, which has a melting point of 3410^{o}C at atmospheric conditions. The substrate holder was placed at a distance of 30 cm from the boat. The thickness of the film was monitored using a quartz crystal thickness monitor. During operation, the substrates were placed into the substrate holder and the bell jar was lowered. The chamber was then pumped down to the required pressure. An ion gauge was used to read the pressure of the chamber. Current was then passed through the boat in order to heat it up. The boat was allowed to heat up for a few minutes, and then the powder was fed onto the boat using the feeding mechanism. Care was taken to ensure that the feed rate of the powder was not very high. The process was continued until the films reached the desired thickness, as read by the crystal thickness monitor. On completion of the deposition process, the current was turned off, and the films were allowed to cool down for 15-20 minutes. Air was then admitted into the chamber, and the films were removed.

A total of seven films were deposited and analyzed. Three of the films were deposited in three different runs, and the four remaining films were deposited in the fourth run. The parameters employed for the deposition process are summarized in table 3. The substrates employed were chosen based on their cost effectiveness. The films grown on the silicon substrates were used only for WDS analysis of the composition of the films. As can be seen in table 3, with each subsequent run, the deposition pressure was lowered.

Table 3. Parameters used in thin film deposition by flash evaporation

Run number	Substrate	Pressure (torr)	Current (A)	Film thickness (Å)
1	Si	1.5×10^{-5}	200	263
2	Si	1.3×10^{-5}	200	1015
3	Si	2.8×10^{-6}	200	800
4	Si, MgO, $SrTiO_3$ and sapphire	2.7×10^{-6}	250	245

C. RESULTS AND DISCUSSION

The films prepared by flash evaporation were analyzed using XRD, EDS, WDS and AFM. The transport properties were not studied, as the WDS studies did not yield encouraging results. The X-ray diffraction patterns obtained from the films grown on various substrates is shown in figures 8,9,10 and 11. From this data, it is seen that amorphous growth occurs on all the substrates. The peaks that are observed in the patterns are a result of diffraction from the substrate on which the film is grown. Hence, we may conclude that the films are not crystalline at all.

Prior to carrying out a detailed WDS analysis of the films, an EDS analysis was carried out. The EDS spectra yielded satisfactory results, in the sense that all the elements that were present in the precursor powder were also present in the film. WDS analysis carried out on the films yielded a Bi:Pb:Sr:Ca:Cu ratio of 2:0.63:0.61:0.35:2.22. The powder that was used to prepare the thin films had the elemental ratio Bi:Pb:Sr:Ca:Cu as 2:0.15:1.96:1.09:2.18. This clearly indicates that the films that are grown using flash evaporation are deficient in Sr and Ca. This is probably because of the limitation of the flash evaporation system itself, in the sense that it was not able to generate a temperature high enough to evaporate all of the material flux arriving at the boat.

On referring to the literature, in was found that successful growth of superconducting BSCCO 2212 thin films by flash evaporation had been achieved by Stolzel et al. [29] who had, however, used exorbitantly high temperatures of almost 2000^{o}C in order to evaporate the powder. The system used in this study was incapable of achieving temperatures of that order. The final run on the system was done using the maximum safely achievable current, which was inadequate to evaporate all the flux arriving at the boat. The WDS analysis also indicated the presence of small amounts of tungsten present in the film.

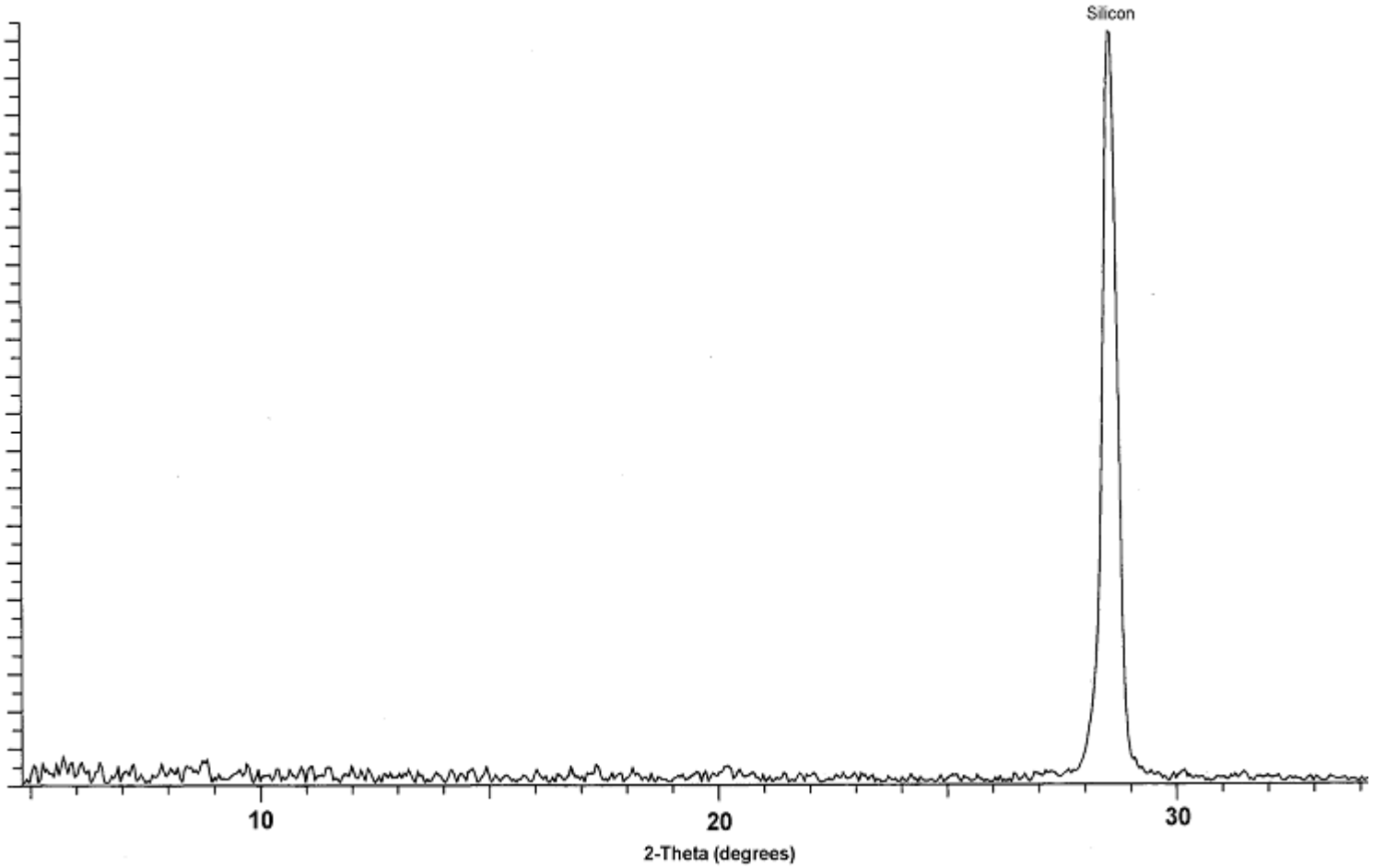

Figure 8. X-ray diffraction pattern of thin film grown on silicon (111) by flash evaporation

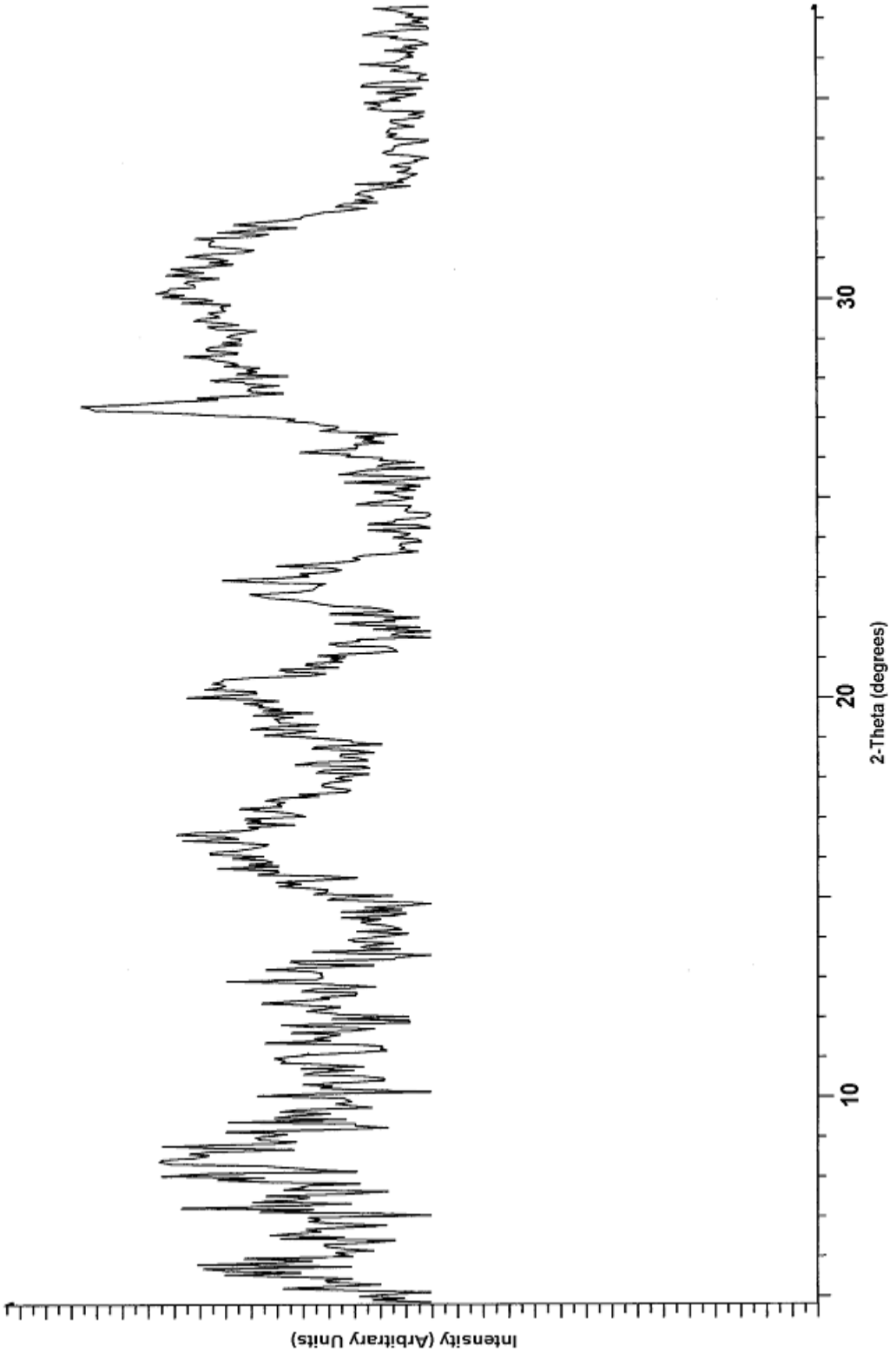

Figure 9. X-ray diffraction pattern of thin film grown on MgO (100) by flash evaporation

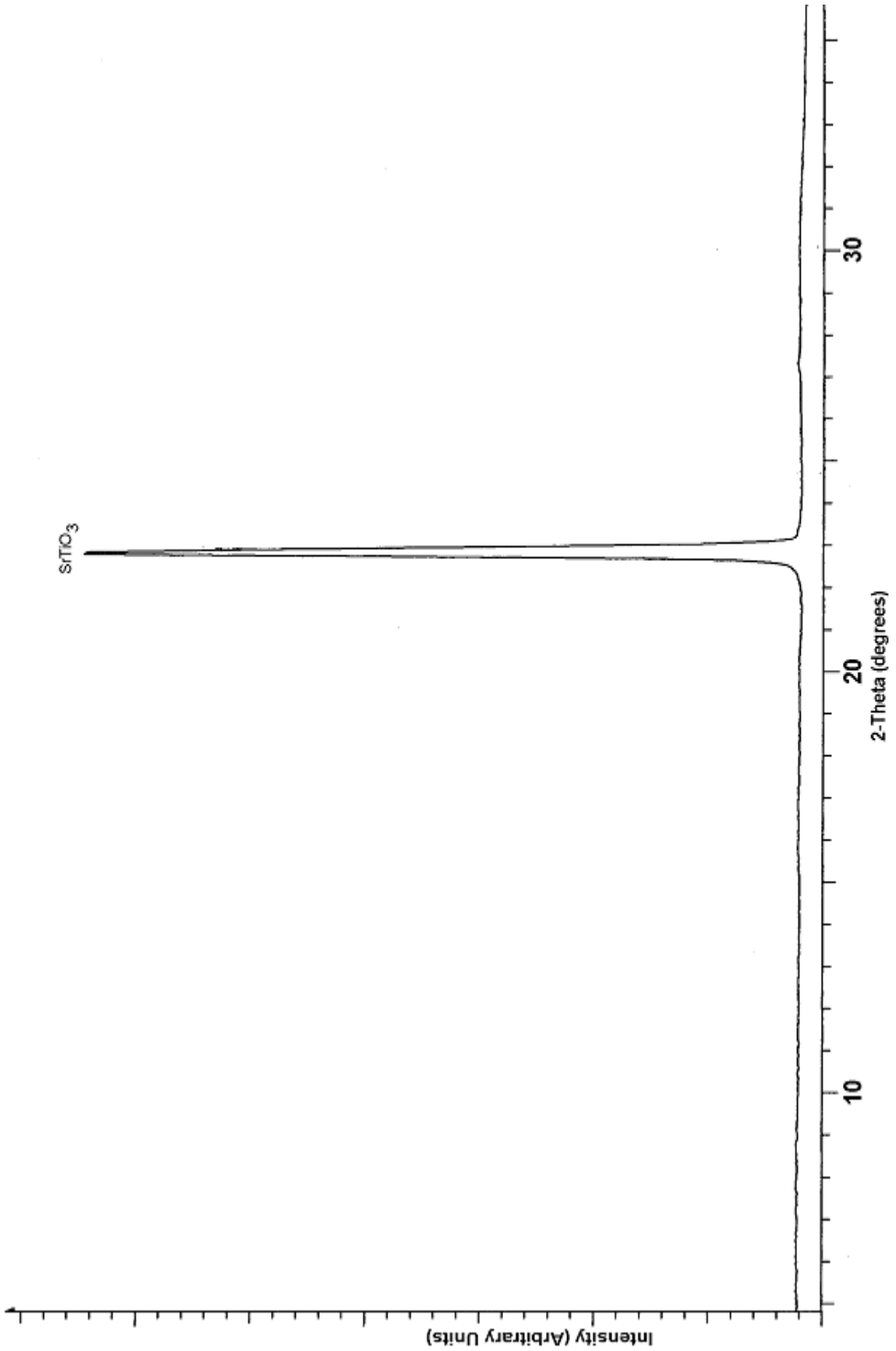

Figure 10. X-ray diffraction pattern of thin film grown on $SrTiO_3$ (100) by flash evaporation

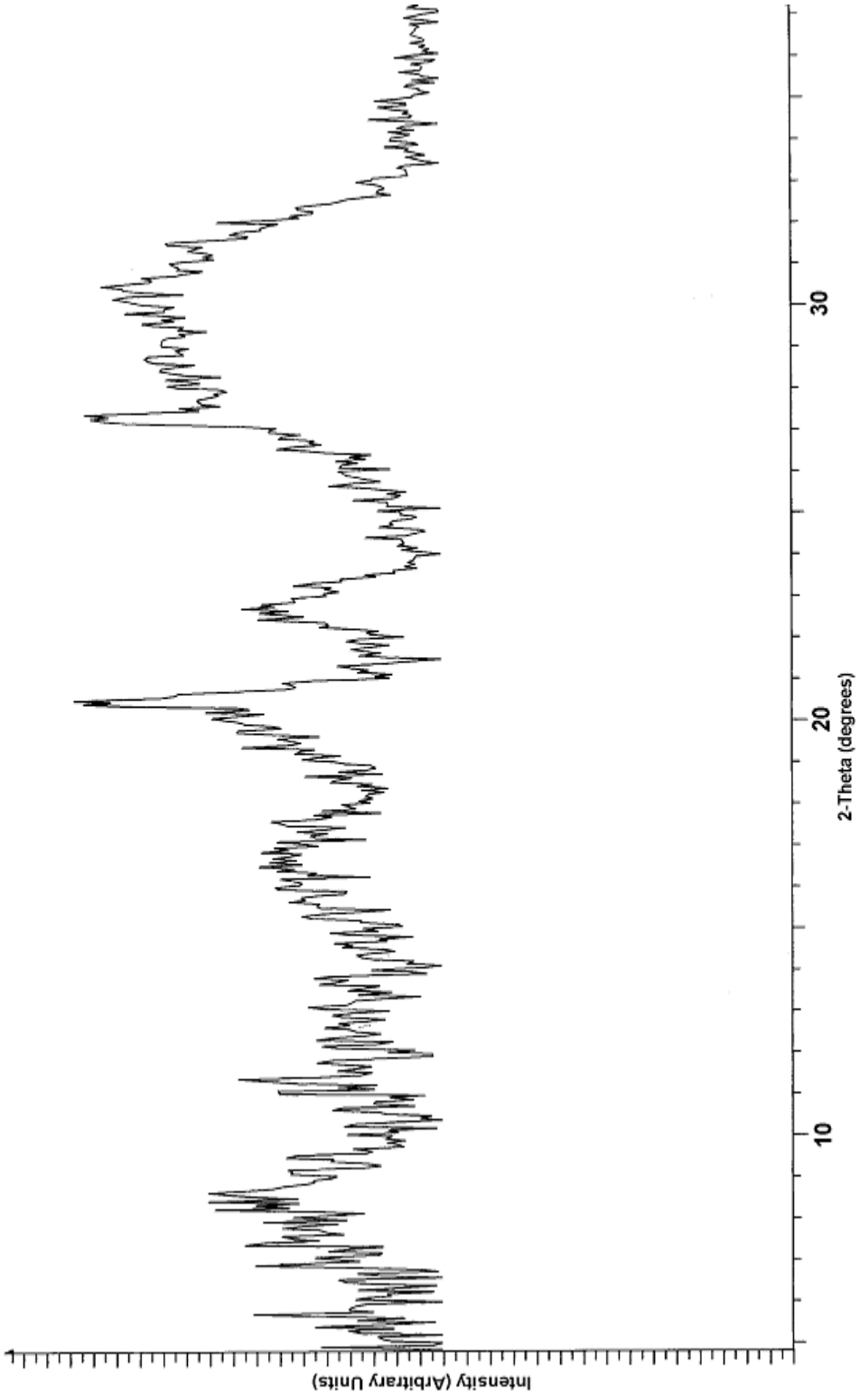

Figure 11. X-ray diffraction pattern of thin film grown on sapphire (0001) by flash evaporation

The surfaces of the films grown by us were analyzed using an AFM in both contact and non-contact mode. The contact mode was preferred, as the sample was found to be immune to the moving of the AFM tip on its surface. Figures 12-14 show images of the thin films grown on various substrates, along with the surface roughness measurements and three-dimensional views. The roughness of the film (the difference between the highest point and the lowest point on the film) was found to be 608 Å for MgO (mismatch=9.91%), 909 Å for sapphire (mismatch=22.25%) and 644 Å for $SrTiO_3$ (mismatch=2.3%) substrates. The largest particle sizes were found to be 1.25 μm for MgO, 0.745 μm for sapphire and 0.47 μm for $SrTiO_3$ substrates. It is seen that as the lattice mismatch increases, the number of particles on the film, and also the surface roughness increase. These results are in agreement with the results obtained by Sato et al. [26].

In conclusion, we may say that flash evaporation is not a very useful technique to grow superconducting thin films of BSCCO, as the temperatures required to achieve the same are exorbitantly high, and there is a chance of contaminating the films with the material of the boat. Further post-deposition heat treatment may be required to increase the degree of crystallinity of the films. The primary issue is that the substrate is maintained at room temperature, which does not allow enough time for the atoms arriving at the substrate to migrate to the minimum energy configurations.

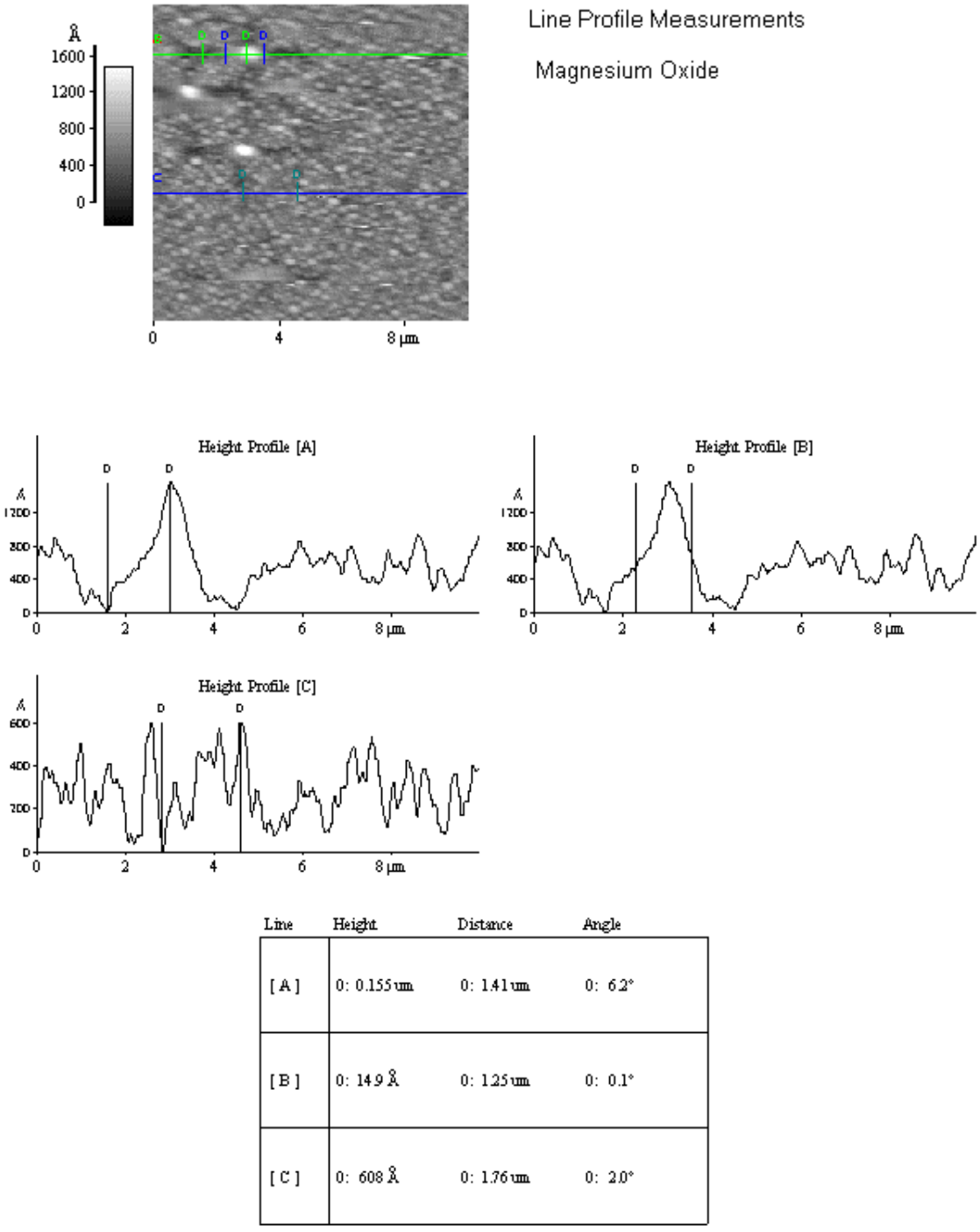

Line	Height	Distance	Angle
[A]	0: 0.155 um	0: 1.41 um	0: 6.2°
[B]	0: 14.9 Å	0: 1.25 um	0: 0.1°
[C]	0: 608 Å	0: 1.76 um	0: 2.0°

Figure 12. AFM measurements on a thin film grown on MgO

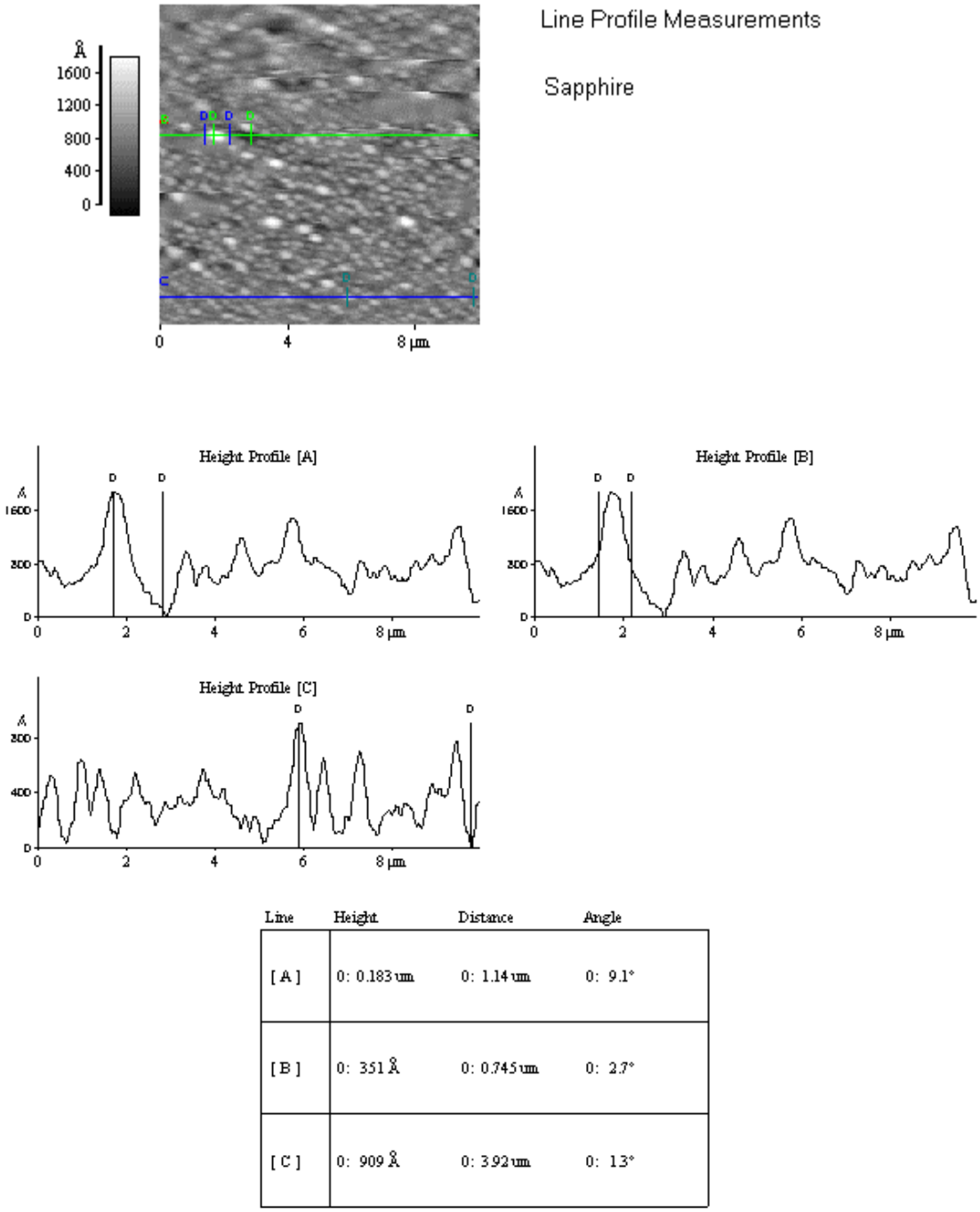

Figure 13. AFM measurements on a thin film grown on sapphire

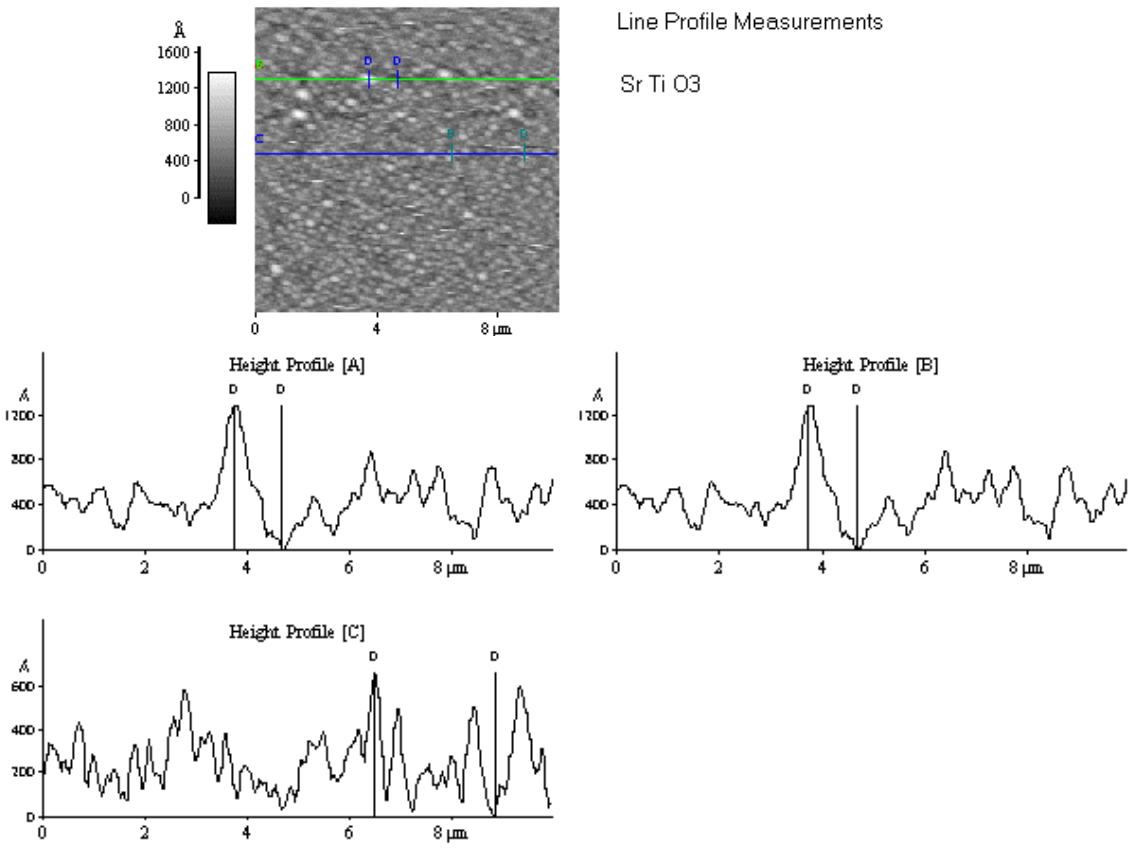

Line	Height	Distance	Angle
[A]	0: 0.128 um	0: 0.941 um	0: 7.8°
[B]	0: 0.128 um	0: 0.941 um	0: 7.8°
[C]	0: 644 Å	0: 2.39 um	0: 1.5°

Figure 14. AFM measurements on a thin film grown on $SrTiO_3$

CHAPTER V
PULSED LASER DEPOSITION*

A. BACKGROUND

The laser is a powerful tool in many applications. It is especially useful in materials processing. Owing to its narrow frequency bandwidth, coherence and high power density, this instrument is used in many research applications. Often the light beam is intense enough to vaporize the hardest and most heat resistant of materials. Besides, due to its high precision, reliability and spatial resolution, it is widely used in the materials processing industry for machining thin films, modification of materials, heat treatment, welding and micro-patterning. Apart from these, polycomponent materials can be ablated and deposited onto a substrate to form stoichiometric thin films. This procedure is referred to as pulsed laser deposition (PLD). The interaction of laser radiation with solid surfaces has been studied as early as 1962, when Breech and Cross [30] analyzed the spectrum of materials vaporized by laser pulses. The first demonstration of PLD [31] did not produce much interest, as the films that were grown were inferior in quality to those grown by CVD and MBE. The technique did not arouse much interest until Dijkamp et al. [32] used PLD to grow films of the high temperature superconducting material $YBa_2Cu_3O_x$ (YBCO). These films were found to be superior in quality to films grown by other techniques, and renewed the interest in PLD as a method of growing thin films.

In principle, the method of pulsed laser deposition is simple. A schematic of PLD is shown in Fig. 15. The setup consists of a vacuum chamber with a quartz window. Inside this vacuum chamber are mounted the target and the substrate.

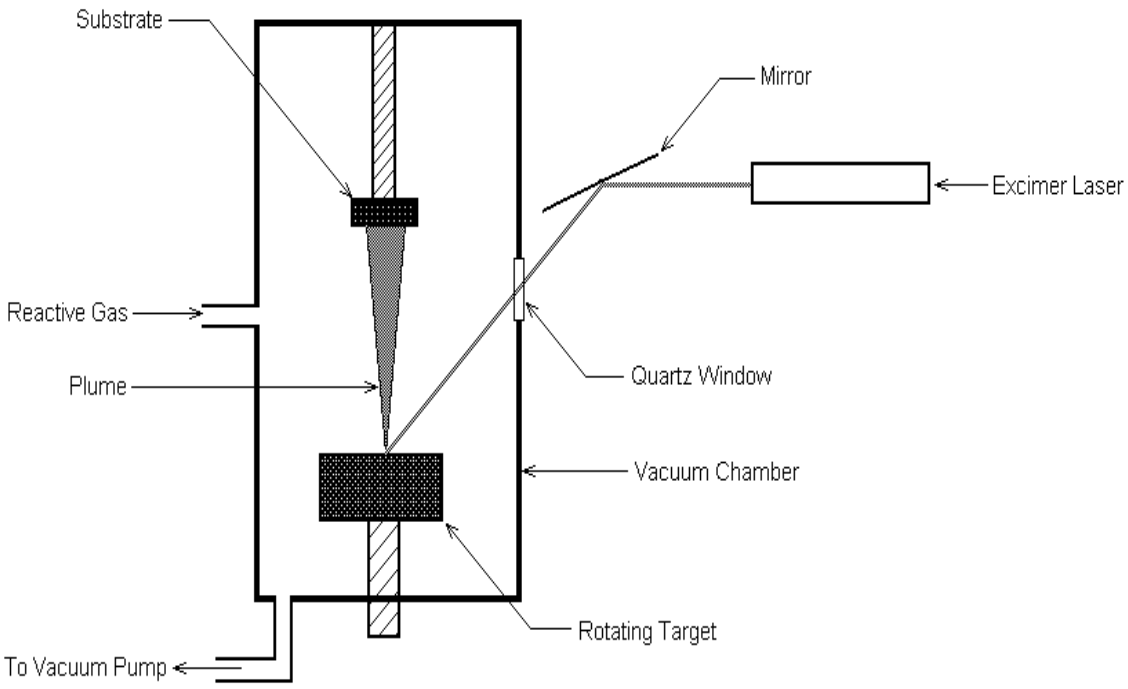

Figure 15. Schematic of pulsed laser deposition

The target is made of the compound that is required to be sputtered, reacted in the solid state and pressed into the form of a pellet using a hydraulic press or some other means. The target and substrate are suitably mounted inside the vacuum chamber. The laser typically has a wavelength of 200nm – 400nm. The most commonly used laser is a Kr-F excimer laser, which has a wavelength of 248 nm [33]. The term excimer stands for excited dimer. These diatomic molecules are composed of one atom of an inert gas, and another of a halogen, and have an extremely short life span and dissociate releasing the excitation energy. The energy density of these lasers is extremely high, typically greater that 1J/cm^2, delivered over an area of 10 mm^2. The energy delivery rate is about 2J/pulse. At these high energies, the frequency is limited to about 30Hz. During the deposition process, the laser is focussed onto the target. The energy is transferred to the target over a very small area, which causes the atoms of the target to evaporate. The constant bombarding of the target by the laser beam results in the formation of a plume. This plume consists of atoms, molecules, ions, electrons, micron-sized solid particulates and molten globules. Film growth occurs on the substrate upon which some of the plume material recondenses. In practice, however, the situation is not so simple, with a large number of variables affecting the properties of the film, such as laser fluence, background gas pressure and substrate temperature. These variables allow the film properties to be manipulated somewhat, to suit individual applications. However, optimization can require a considerable amount of time and effort. Indeed, much of the research into PLD is concentrated on the empirical optimization of deposition conditions for individual materials and applications. The PLD process has numerous advantages. Targets used in PLD are small compared with other targets used in other sputtering techniques. It is quite easy to produce multi-layer film composed of two or more materials. Besides, by controlling the number of pulses, a fine control of film thickness can be achieved. The

deposition rate that can be achieved is of the order of hundreds of angstroms per minute. The fact that the laser is used as an external energy source results in an extremely clean process without the use of filaments. The most important feature of PLD is that the stoichiometry of the target can be retained in the deposited films. This is the result of an extremely high heating rate of the target surface (108 K/s) due to pulsed laser irradiation. It leads to the congruent evaporation of the target irrespective to the evaporating point of the constituent elements or compounds of the target. And because of the high heating rate of the ablated materials, laser deposition of crystalline films demands a much lower temperature than other film growth techniques. For this reason, the semiconductor and the underlying integrated circuit are saved from thermal degradation. In spite of mentioned advantages of PLD, some shortcomings have been identified in use of this deposition technique. One of the major problems is the splashing or the particulates deposition on the film. The physical mechanisms leading to splashing include the surface boiling, expulsion of the liquid layer by shock wave recoil pressure and exfoliation. The size of particulates may be as large as a few microns. Such particulates will greatly affect the growth of the subsequent layers as well as the electrical properties of the film and should be eliminated. Another problem is the narrow angular distribution of the ablated species, which is generated by the adiabatic expansion of laser produced plasma plume and the pitting of the target surface. These features limit the use of PLD in producing a large area of uniform thin film, and PLD has not been fully deployed in the industry. Remedial measures, such as inserting a shadow mask to block off the particulates and rotating both target and substrate in order to produce a larger uniform film, have been developed to minimize some of the PLD problems. As-deposited films are sometime amorphous [34], and require some mode of heat treatment to make them crystalline. The heat treatment can be performed in a separate enclosure after the deposition has been carried out, or can be performed within the deposition

chamber itself. The latter process is called in-situ annealing. The films may either be quenched or slowly cooled down after the heating is done, and each of these processes results in different properties of the films. In the annealing process, the films are heated typically to the range of 800-900^{o}C in an atmosphere of oxygen mixed with an inert gas such as argon. The concentration ratio is typically the same as that used during deposition. This causes the homogenization of the oxygen within the film and causes a more complete filling of the oxygen sites in the lattice. The argon is required to ensure a high annealing overpressure, so that the films do not evaporate. Experiments have shown that phase formation does not begin until about 600^{o}C. At these temperatures, the 2201 phase is formed. The 2212 phase does not begin to form until a temperature of 800-820^{o}C is reached [34]. After 880^{o}C, however, the films begin to melt away and burn. It is theorized that longer anneal times at higher temperatures drives the calcium atoms to the 2201 phase, where there exists a deficiency of calcium, thereby forming the 2212 phase. At a much longer annealing time, however, the calcium ions, having a lower vapor pressure, would tend to evaporate, thereby converting the 2212 phase back into the 2201 phase. The rate of heating and cooling also has an effect on the sample qualities. Rates of heating and cooling as high as 260^{o}C/min and 80^{o}C/min respectively, and as low as 28^{o}C/min and 9^{o}C/min respectively, have been investigated [35]. It was observed that the high heating and cooling rates result in the films having a large width of superconducting transition, indicating that the current is either transported through multiple superconducting phases, or through very poorly coupled grains of a single phase. SEM micrographs of the two films indicate that slow heating and cooling promotes a larger grain size, whereas rapid heating and cooling will produce a grain size about one-fifth the size of the former. Rapid heating and cooling produces unidentified secondary phases, in the form of rod-like structures. Another interesting development is that in a sample that is rapidly heated and cooled, the center of the samples have better developed 2212

phases than the periphery, which is more evidence that a slow rate is required for the development of the 2212 phase. X-ray diffraction of these two kinds of samples reveals the presence of multiple extraneous phases in samples that were rapidly heated and cooled. Another method of growing the films involves the use of a heated substrate. In this method, post-deposition annealing is not required. This process also provides energy to the different species that land on the substrate and allows them to migrate to the minimum energy configurations. Films grown in this way have shown the presence of the superconducting phases without post-deposition annealing [36]. Epitaxial growth has also been observed in films grown by this method [37] by using a substrate temperature as high as 830-840^{o}C.

B. GROWTH OF BSCCO THIN FILMS

The PLD of thin films of BSCCO was carried out by part of our research group affiliated with the Institute for Superconducting and Electronic Materials (ISEM) at the University of Wollongong, Australia. The laser used was a KrF excimer laser, having a wavelength of 248 nm. The beam energy was focussed onto the target to obtain an energy density of 3.25 J/cm^2. The frequency of pulsing of the laser used was 2 Hz. The substrate used was single-crystal MgO, The target used was made using commercially obtained BSCCO 2212 powder, pressed into the form of a pellet using a pressure of 17 tons. This pellet was then annealed at 847^{o}C for 20 hours. The substrate-target distance was 55 mm. Prior to deposition, the substrates were cleaned in acetone in order to remove any traces of impurities and then washed in de-ionized water. The substrates were then mounted onto the substrate holder using silver paste. Before commencing the deposition process, the substrate was heated to a temperature of 800^{o}C in an atmosphere of pure oxygen. It was maintained at this temperature for 30 minutes and then cooled

Table 4. Temperature of deposition and T_C of various films of BSCCO grown by PLD

Film deposited at (^oC)	**T_C (K)**
A. 700	43
B. 725	58
C. 735	63
D. 750	63

down to the deposition temperature. This was done in order to remove any trace impurities that might be present. The target was ablated for 10 minutes in order to reach a steady state of material flux from the target, and the deposition was carried out for 30 minutes. The gas used during the deposition was pure oxygen at a pressure of 100 mTorr. After deposition, the films were in-situ annealed at 760^{o}C for 30 minutes at 500 torr oxygen pressure. They were then cooled down to room temperature in 30 minutes. The thickness of the films obtained by this method was found to be 400 nm. A total of 4 films were grown by this method. They were grown at deposition temperatures of 700^{o}C, 725^{o}C, 735^{o}C and 750^{o}C. In order to study the effect of annealing on the T_c of the films, the film grown at 735^{o}C was passed through various annealing cycles in atmosphere of 90% oxygen and 10% argon. In the first cycle, it was annealed at 825^{o}C for 1 hour. In the second cycle, it was annealed at 835^{o}C for one hour. In the third cycle, it was annealed at 835^{o}C for three hours. In order to study the effect of annealing on the phase of the film, the film grown at 725^{o}C was passed through two annealing cycles, the first at 825^{o}C for two hours, and the second at 825^{o}C for three hours.

C. RESULTS AND DISCUSSION

The thin films of BSCCO that were grown using PLD were characterized for their physical and transport properties. The AC susceptibility was determined using a physical properties measurement system magnetometer and was used to determine the T_C of the films. The physical properties were studied using AFM, SEM and XRD. Table 4 shows the T_C of the various films, and figure 16 shows the results of AC susceptibility measurements on the thin films. We define sharpness of transition as the difference between T_C(onset) and T_C(zero). We also define T_C(zero) as the temperature at which the parameter used to

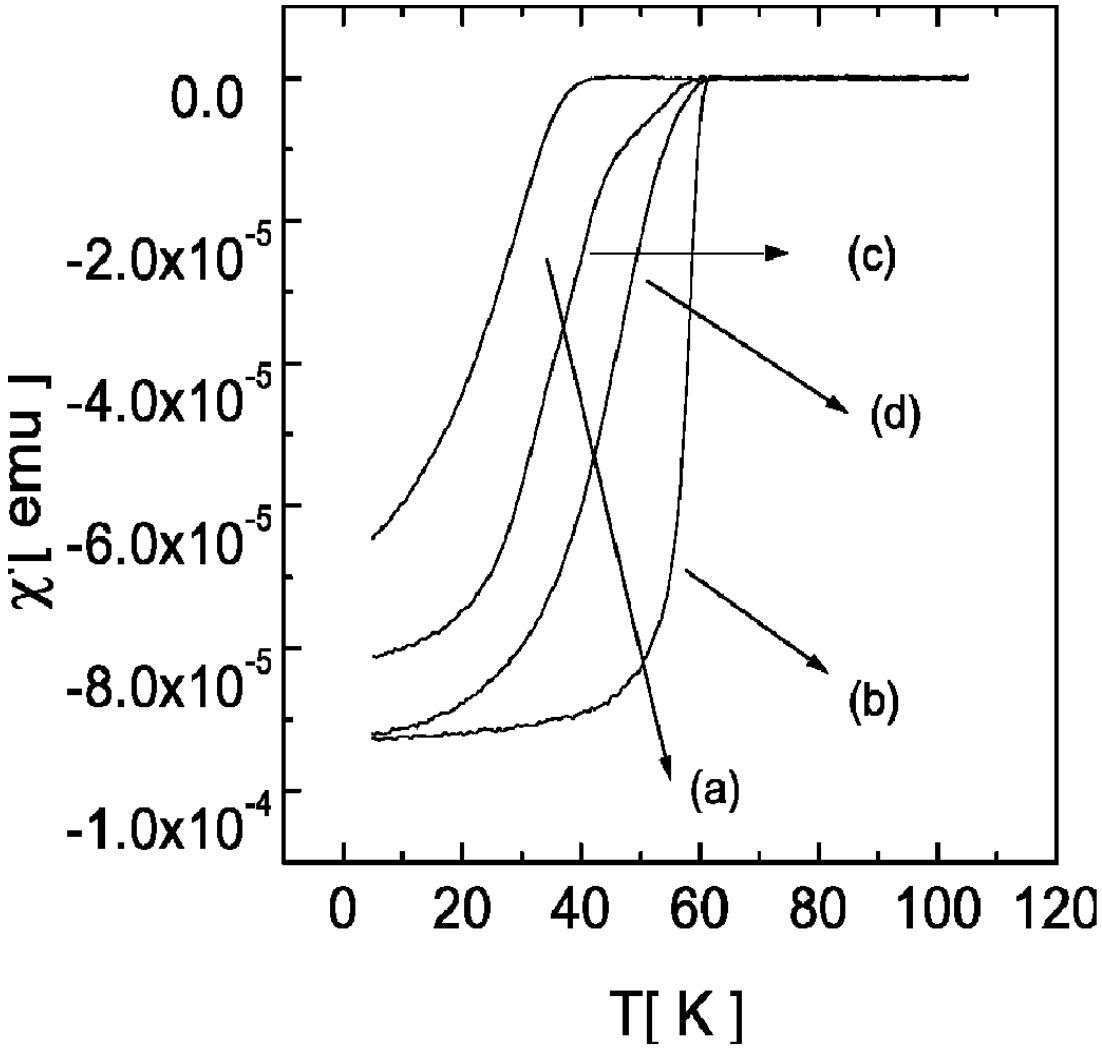

Figure 16. AC susceptibility of BSCCO thin films grown by PLD at (a) 700^{o}C (b) 725 ^{o}C (c) 735 ^{o}C (d)750 ^{o}C

characterize T_C is 10% in excess of the difference in its values at T_C(onset) and at temperatures below 20 K. We see that film (b), grown at a temperature of 725^{o}C displays a sharpness of transition of 10 K, which is lesser than the best results we have seen, namely 11 K obtained by Ishii et al. [38] and 13 K obtained by Matthiesen et al. [35].

In order to study the effect of annealing on the films, one of the films, namely the one deposited at 735^{o}C, having an as-deposited T_C of 63 K was chosen for annealing. The results of annealing this film are shown in figure 17. The film was annealed at 825^{o}C for one hour and the T_C was measured. There was no appreciable increase in the T_C, but the slope of the transition had become steeper. The film was then annealed again at 835^{o}C for another hour. It was found upon the second run of annealing that the transport characteristics of the film changed, and started resembling that of the as-deposited film. This film was then annealed one more time at 835^{o}C for 2 hours. It was found that the T_C of the resulting film had increased to 71 K, but the sharpness of the transition was lost. The initial increase in the sharpness of the superconducting transition indicates that the superconducting domains that are present in the film get coupled better, increasing the homogeneity of the film. As the film is further annealed, the sharpness is lost, which indicates that the percentage of the 2212 phase is diminished with larger annealing times.

The film that was grown at 725^{o}C, having an as-grown T_C of 58K was chosen to study the effect of annealing times by X-ray diffraction. The X-ray diffraction pattern of the as-grown film was first recorded. The film was then annealed at 825^{o}C for 2 hours and the X-ray diffraction pattern of the resulting film was recorded. The film was then annealed once more at 825^{o}C for 3 hours and the X-ray diffraction pattern was recorded again. The results of the X-ray diffraction are shown in figure 18.

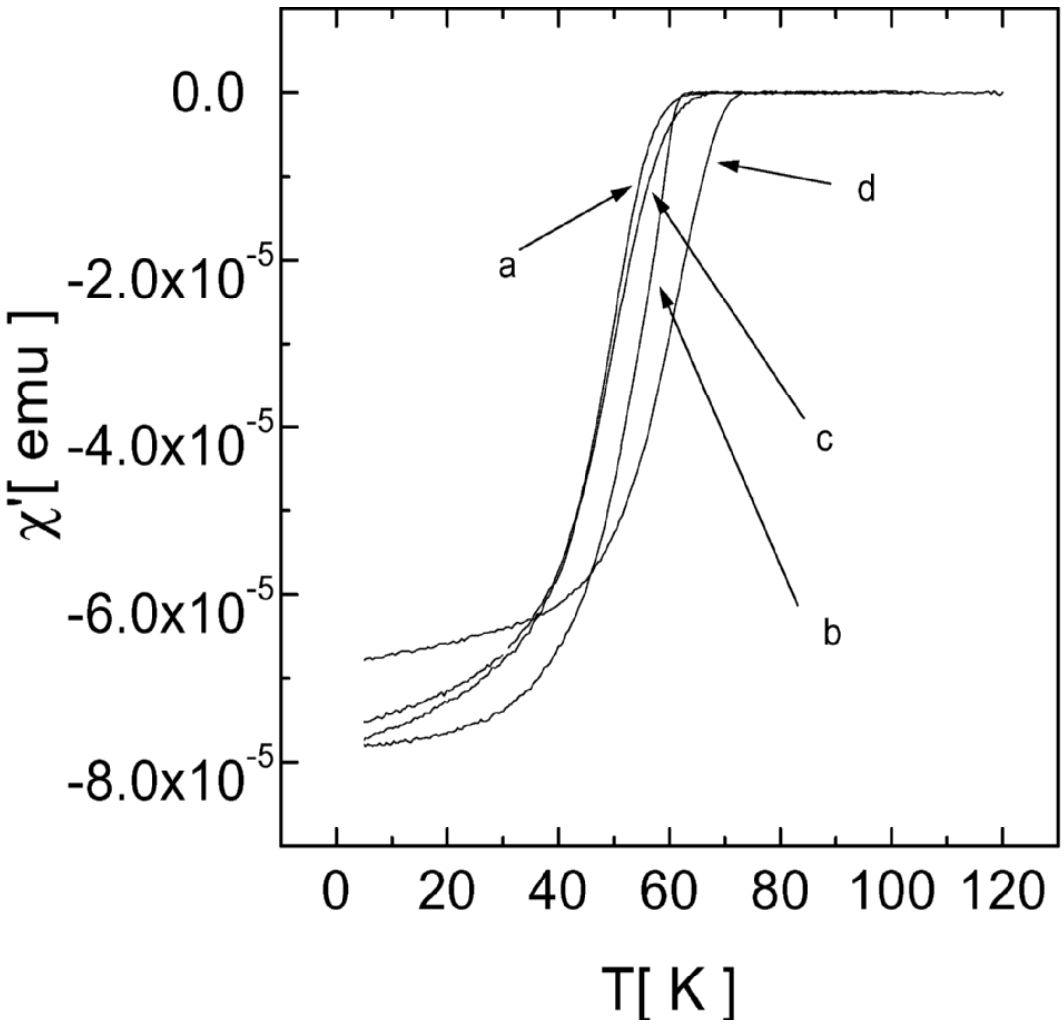

Figure 17. Effect of annealing on (a) As-grown film deposited at 735^{o}C (T_C=58K) (b) Annealed at 825^{o}C for 1 hour (T_C=63K) (c) Annealed at 835^{o}C for 1 hour (T_C=63K) (d) Annealed at 835^{o}C for 2 hours (T_C=71K)

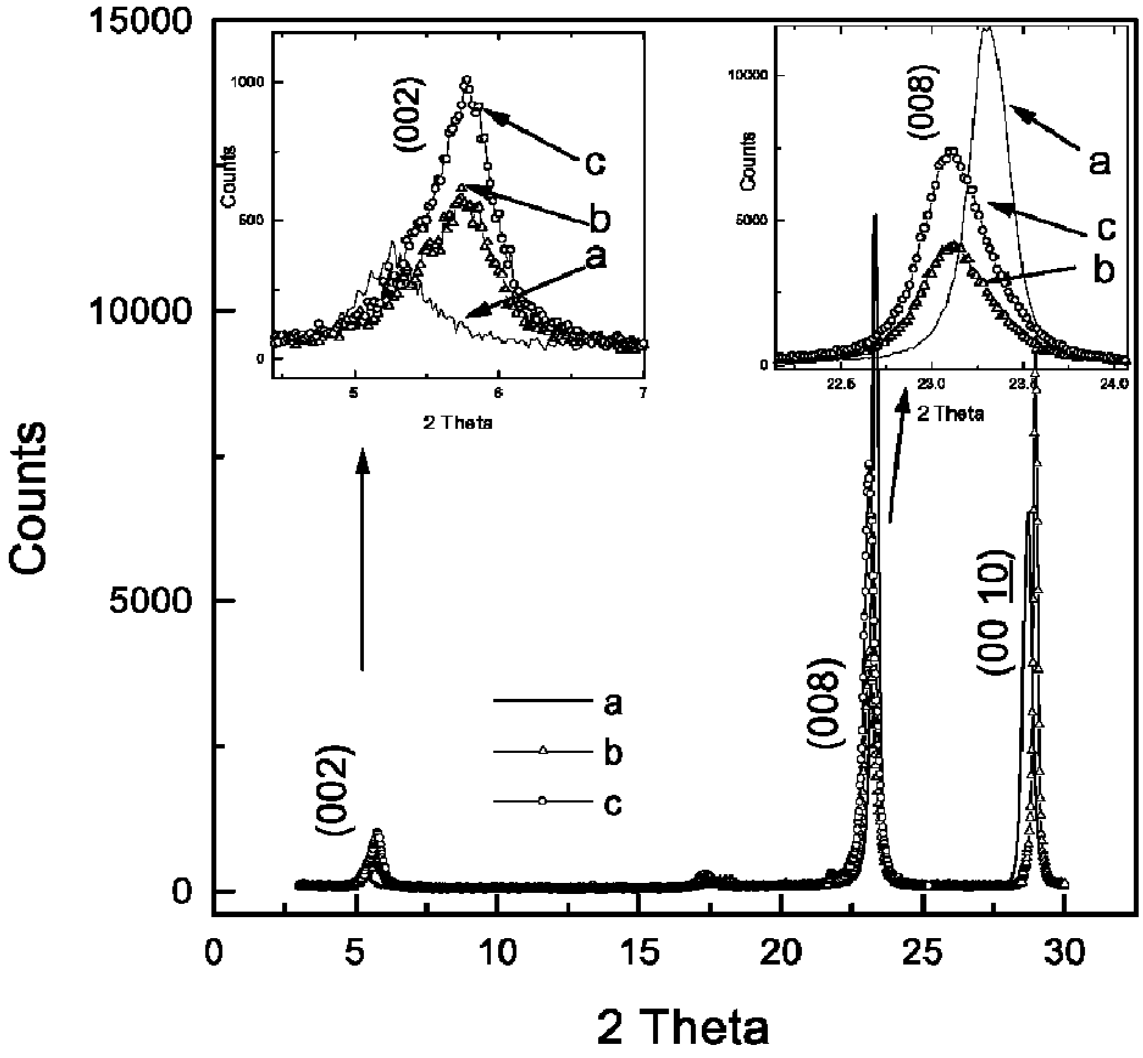

Figure 18. Effect of annealing on (a) As-grown film (T_C=63K) (b) Annealed at 825^{o}C for 2 hours (c) Annealed at 825^{o}C for 3 hours

The only peaks visible on the X-ray diffractogram were the peaks corresponding to the (00l) planes of BSCCO 2212 [10]. We conclude that the film is c-axis oriented and comprised wholly of the 2212 phase. The film that was annealed at 825^{o}C for two hours shows a slight angular shift of the X-ray diffraction peaks. There is no consistent increase or decrease in the intensity of the peaks with longer annealing time. There is, however, an angular shift of the peaks which suggests that the films re-crystallize [38] because of annealing. There is also a broadening of the peaks with increasing annealing time. This, in connection with the angular shift of the peaks, is suggestive of the fact that grain growth of the 2212 phase occurs. This introduces local strains, and the lattice mismatch between the substrate and the film relatively increases, resulting in broadening of the peaks. The angular shift also indicates a change in the oxygen content of the film.

The film grown at 725^{o}C was also characterized using AFM before and after annealing, and the results are shown in figure 19. The difference between the highest and lowest points on the film was takes to be a measure of the roughness. For the as-grown film, a value of 250 nm was obtained, as opposed to 100 nm for the annealed film. It is seen that annealing for short periods of time significantly reduces the roughness of the films. Before annealing, this film was also characterized using SEM, and it was seen that the largest particle size was less than 300 nm.

In order to study the effects of exposure of the thin films to prolonged high temperatures, another film, the one grown at 735^{o}C was annealed for 20 hours at 835^{o}C in an atmosphere of 10% argon and 90% oxygen. This film was then characterized using AFM and XRD.

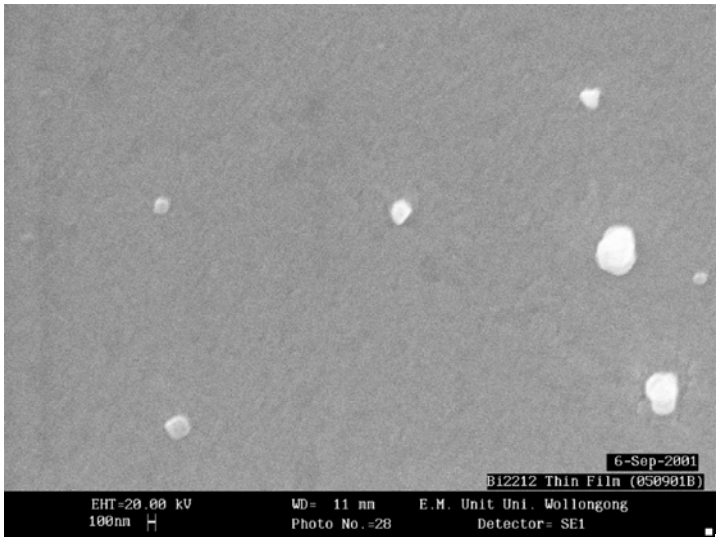

(a)

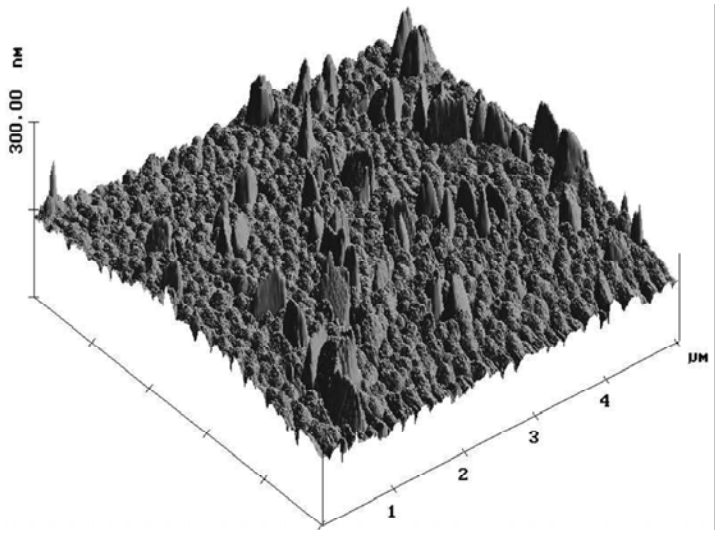

(b)

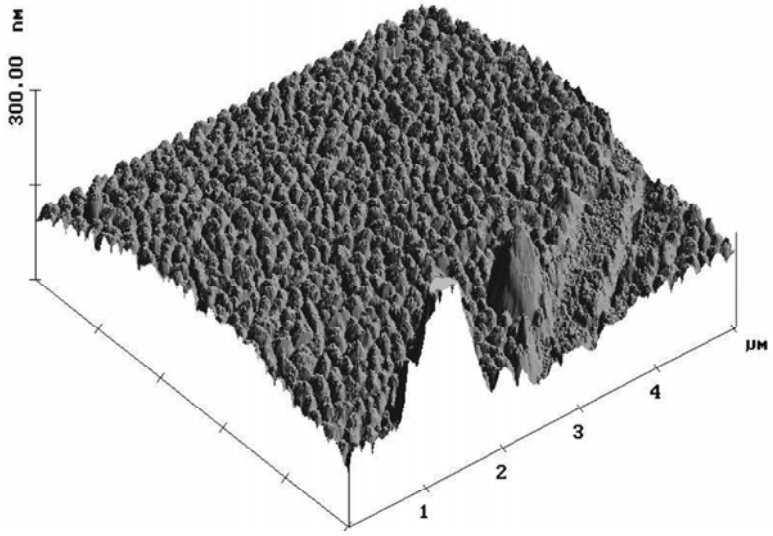

(c)

Figure 19. (a) SEM micrograph of as-grown film, grown at 725^{o}C
(b) AFM image of the above film
(c) AFM image of the film, annealed at 835^{o}C for 1 hour

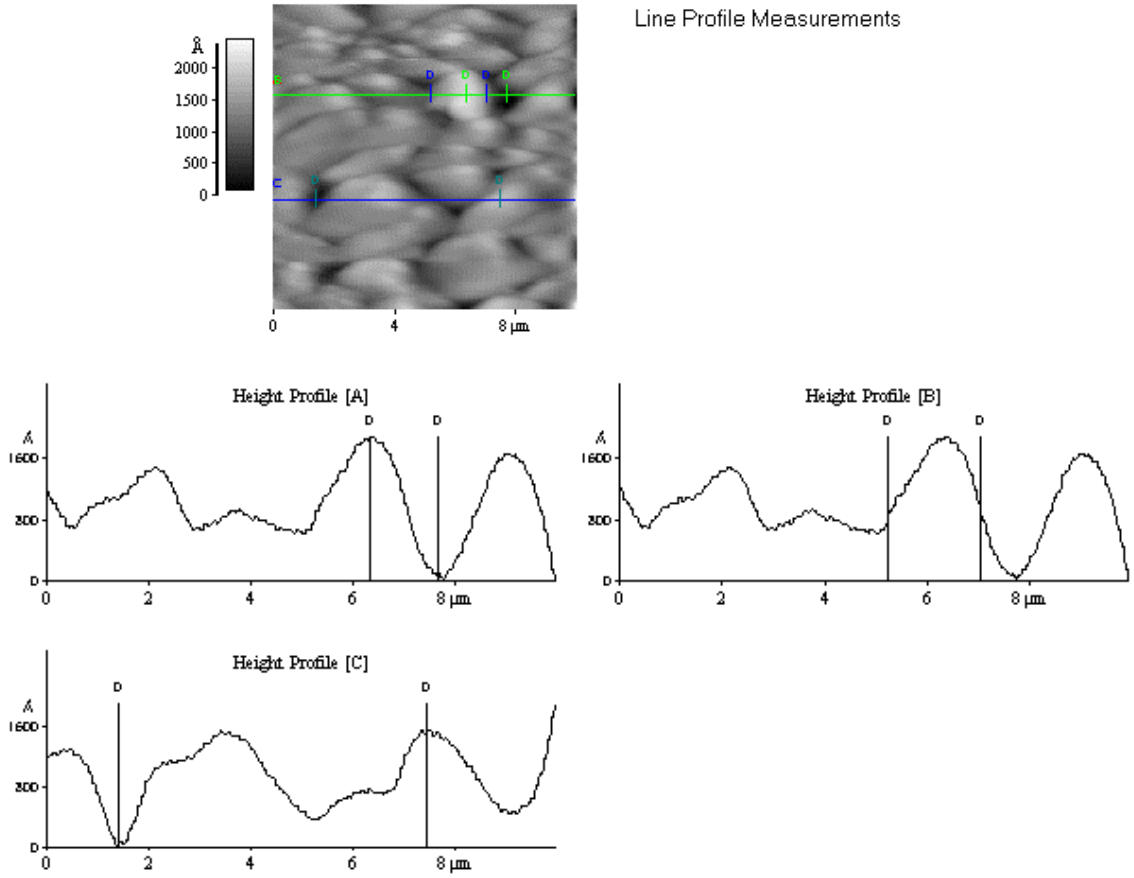

Line	Height	Distance	Angle
[A]	0: 0.181 um	0: 1.33 um	0: 7.7°
[B]	0: 65.2 Å	0: 1.84 um	0: 0.2°
[C]	0: 0.150 um	0: 6.08 um	0: 1.4°

Figure 20. AFM analysis of BSCCO thin film annealed for 20 hours at 835^{o}C

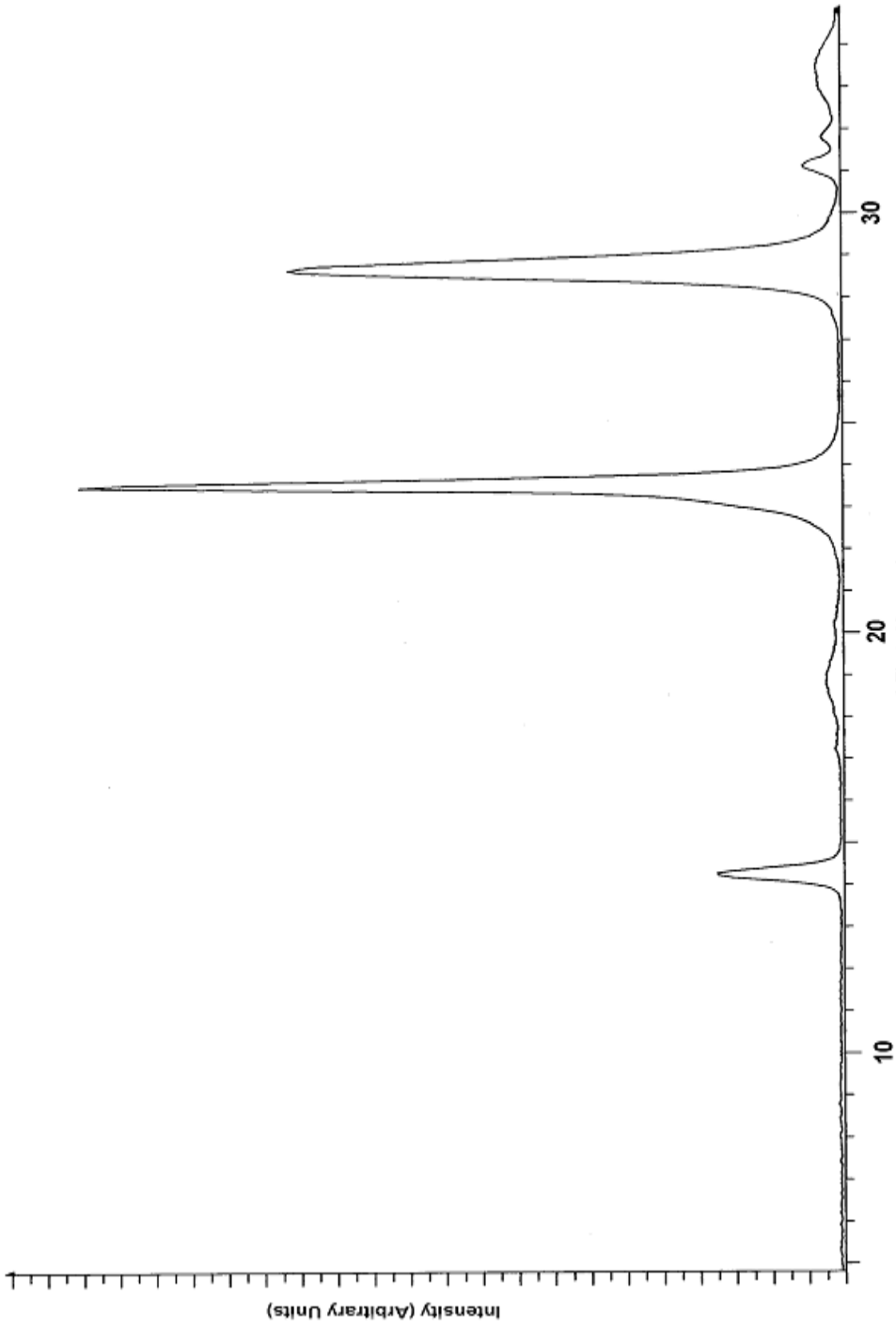

Figure 21. X-ray diffraction pattern of a BSCCO thin film grown by PLD annealed for 20 hours

The results of the X-ray diffraction and AFM are shown in figures 20 and 21. From the XRD pattern of the film, it is seen that there is a large angular shift of the peaks. A new peak, corresponding to the 2201 phase is observed [39] at about 14 degrees. This indicates that the 2212 phase decomposes into the 2201 phase upon prolonged periods of annealing. From the AFM data obtained, it is seen that the surface roughness is 0.18 μm as opposed to less than 0.1 μm for the films annealed for short periods.

CHAPTER VI
OTHER TECHNIQUES

A. MOLECULAR BEAM EPITAXY

Molecular beam epitaxy, or MBE for short, was developed in the early 1970's as a means for growing high quality thin films [40]. It is one of the best techniques for controlling the film quality, geometry and doping. It is also one of the most expensive and time-consuming methods of growing thin films. The primary constituent of an MBE setup is a Knudsen cell, or effusion cell. This cell is a resistively heated cylinder that contains the element to be deposited. For a multi-component film, multiple cells are used. These cells have a very narrow opening for the vapor of the species to effuse out of. They are also equipped with a shutter in order to initiate and terminate the flux of the species. One of the important parameters in MBE is the mean free path of the atoms that are to be deposited. The expression for the Mean Free Path is given by [41]

$$\lambda = (n\pi\sigma^2/V)^{-1}$$

Where λ = Mean Free Path
n = Number of atoms present in chamber
V = Volume of chamber
σ = Diameter of atoms

The substrate is located at such a point in the chamber that the distance from the substrate to the effusion cells is less than the mean free path of the effusing species. This distance varies from 5-30 cm, depending on the pressure. In order to grow oxide thin films, instead of elemental thin films, pure oxygen or ozone gas is introduced into the deposition chamber. A schematic of the process is shown in figure 22.

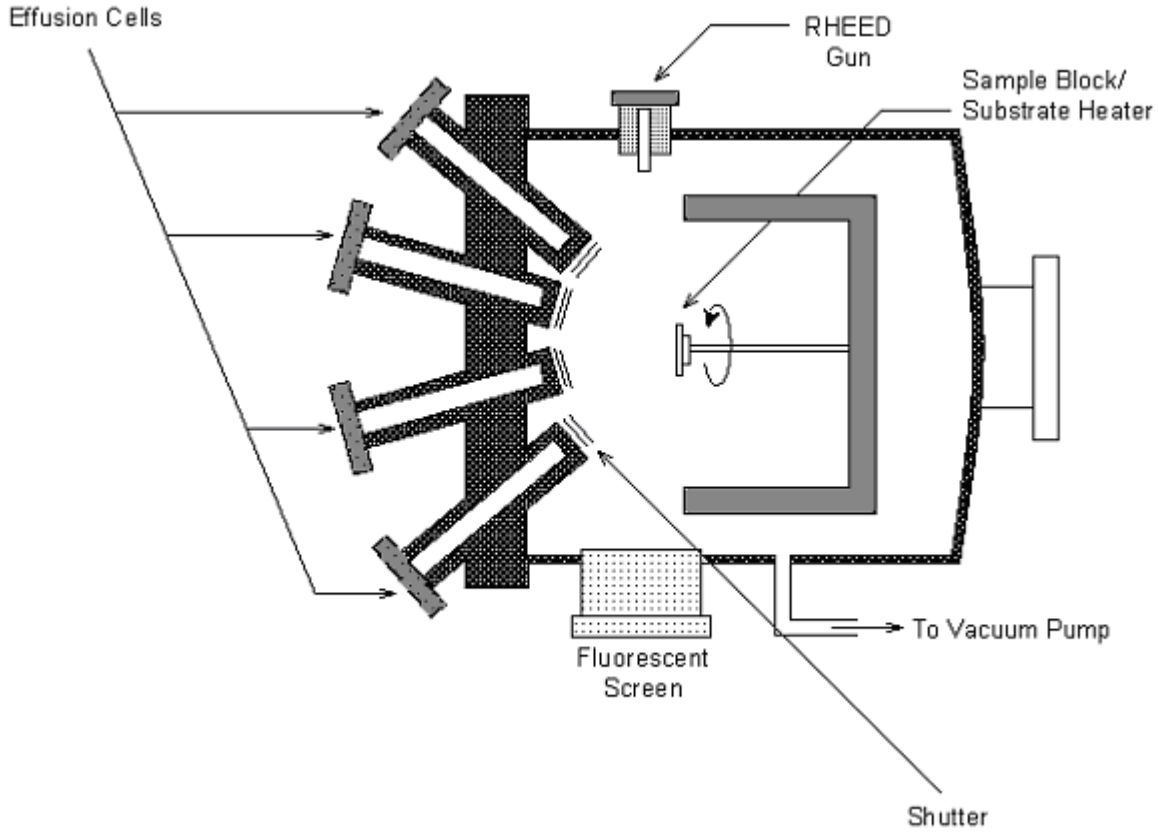

Figure 22. Schematic of molecular beam epitaxy

B. SPUTTERING

There are various types of sputtering, namely DC sputtering, RF sputtering, magnetron sputtering, reactive sputtering, and hybrids of the above processes. The main principle is illustrated in figure 23 [42].

In the sputtering process, the target is composed of the metal, whose oxide is required to be deposited on the substrate. A voltage bias is maintained between the target and the substrate. The deposition chamber is evacuated, and the process gas is injected into the chamber. The process gas is typically a noble gas mixed with oxygen. The target is maintained at a negative voltage. As the voltage between the substrate and the target is increased, the process gas gets converted into high-energy ions. These ions are attracted to the negatively charged target, bombard it, and knock off atoms from the target. These target atoms react with the oxygen present in the chamber and form their respective oxides. These oxides are electrically neutral, and are, essentially, a vapor. This vapor deposits itself onto the surface of the substrate in the form of a thin film.

The sputtering process suffers from a disadvantage that the sputter yield of the different elements that comprise the target is different, and hence the stoichiometry of the film obtained is different from that of the target. The substrate also gets heated up during the deposition process due to bombardment by the sputtering gas [43]. This heating of the substrate is beneficial, in the fact that it provides energy to the incident atoms to migrate along the surface of the substrate and find the minimum energy positions. If, however, the substrate gets too hot, it will cause the surface atoms to evaporate, leading to a low deposition rate, or even etching of the substrate. In order to sputter-deposit thin films of insulating materials, exorbitantly high DC voltages are needed. In order to bypass this, a RF voltage is applied between the target and the substrate. The frequency of the current is in the range of 5 to 30 MHz.

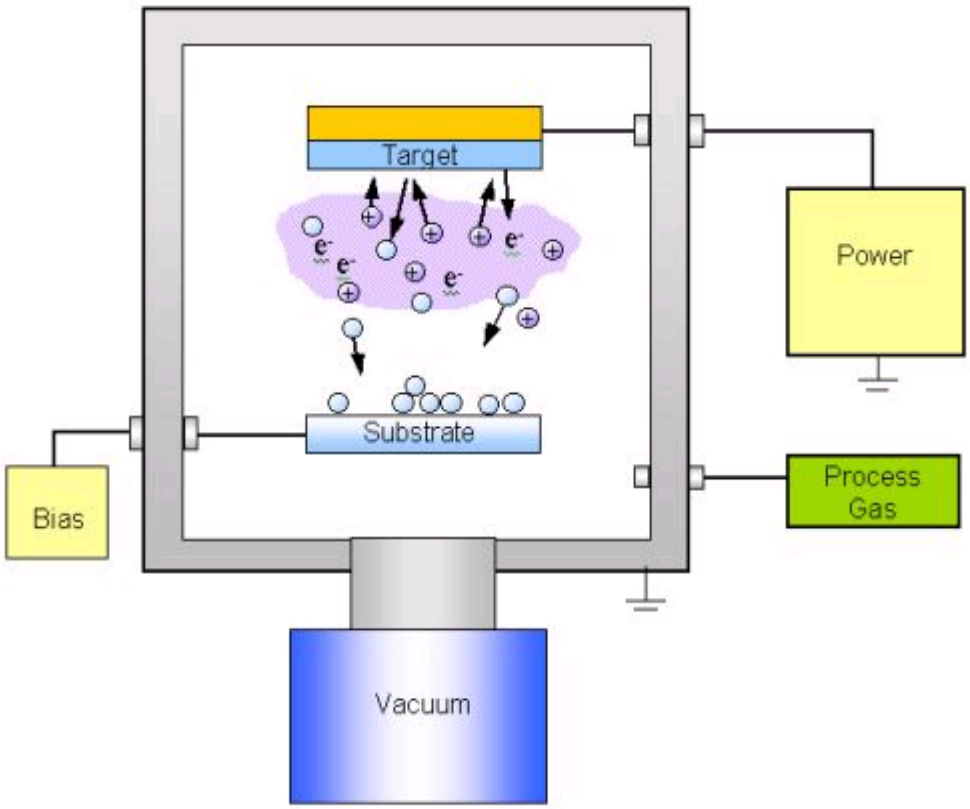

Figure 23. Schematic of the sputtering process

Another variation of sputtering is magnetron sputtering. In this process, a magnetic field is used in addition to the electric current. The magnetic field is applied just above the target. This causes electrons to stay near the target, and not migrate off towards the substrate. This leads to higher ionization efficiency of the plasma near the target, and hence leading to higher deposition rates. One of the primary advantages of sputtering lies in the fact that it can be used to clean the substrate before deposition. In this process, the polarities are reversed so that substrate plays the role of the target, and when a current is passed, the substrate gets bombarded by the inert gas ions and is etched.

CHAPTER VII
CONCLUSION

Being able to produce high quality films of the bismuth high T_C family is a difficult task and single phase 80K or 110K thin films is an elusive goal that will require much research. When dealing with systems with the degree of complexity of this one, it is often difficult to precisely understand how to improve the quality of the thin films. The lack of a strong theoretical model further hampers all attempts to efficient and economic production of thin films of good quality. It has been found that the temperature of deposition plays a critical role in the transport and structure characteristics of the film. Also, the post deposition annealing plays a very important role in determining the final properties of the film.

Although it has its own merits, flash evaporation has not proved to be a very efficient technique for deposition of BSCCO thin films. With higher deposition temperatures, however, flash evaporation might produce better results, but the danger of particles from the heating element being present in the film presents itself. Flash evaporation, however, produces a very large area of deposition. In our experiments, we have found that the area of deposition is in excess of 150 cm^2. Furthermore, flash evaporation does not require the substrate to be heated in any manner. This would mean that in the fabrication of integrated circuits, there would not be any diffusion-related damage to the circuit, as the substrate is maintained at room temperature. However, precisely the same characteristic of flash evaporation proves to be its downfall, since the atoms arriving at the surface of the substrate condense immediately, and have no time to migrate to the minimum energy configurations.

Pulsed laser deposition, on the other hand, has proved to be a most useful technique for growing thin films of BSCCO. We have overcome the barrier of having multiple phases within the same film by using this method, and have

produced one of the sharpest transitions from the non-superconducting state to the superconducting state. This sharp transition is necessary for electronic devices, as it would result in a higher speed of operation. PLD, however, suffers from its own drawbacks. The area of the films grown was a meager 9 mm^2, which took half an hour of deposition time. Assuming 18 mm^2/hour as the average deposition rate, in order to grow films on a 4 cm x 4 cm substrate, which is the size of a typical microprocessor chip, it would take in excess of 80 hours, or in excess of 3 whole days. This shows that PLD is not a time-effective method of growing large areas of thin films. However, the possibility of multiple laser beams and multiple targets has not yet been considered, and might be a direction of research worth pursuing, in order to grow thin films more time-effectively. There still remains the problem of eliminating the particles being present on the surface of the thin films, which is a direction for further research.

REFERENCES

1. H. Maeda, Y. Tanaka, M. Fukutomi, T. Asano, Jap. J. Appl. Phys., 27 (1988) L209
2. K. Onnes, Akad van Wetenschappen 14 (1911) 818
3. W. E. Hatfield in: High Temperature Superconducting Materials, Eds. W. E. Hatfield and J. H. Miller Jr., Marcel Dekker, New York, 1988 p. 39.
4. K.W. Goeking, PhD Dissertation, 1990, Texas A&M University
5. C. W. Chu, P. H. Hor, R. L. Meng, L. Gao and Z. J. Huang, Science 58 (1987) 567
6. C. Wang and C. W. Chu, Phys. Rev. Lett. 58 (1987) 908
7. J. Bardeen, L. N. Cooper and J. R. Schrieffer, Phys. Rev. 106 (1957) 162.
8. W. Meissner and R. Ochsenfeld, Naturwissenschaften 21 (1933) 787
9. A. A. Abrikosov, Sov. Phys., J. Expt. Theo. Phys. (JETP) 5, (1957) 1174
10. E. Takayama-Muromachi, Y. Uchida, Y. Matsui, M. Onada and K. Kato, Jpn. J. Appl. Phys. 27 (1988) L556
11. M. Yavuz, H. Maeda, L. Vance, H.K. Liu, S.X. Dou, J. Alloys and Cmpds. 281 (1998) 280
12. S. Koyama, U. Endo and T. Kawai, Jap. J. of Appl. Phys. 27 (1998) L1861
13. W. Kula, R. Sobolewski, J. Gorecka and S.J. Lewandowski, J. of Appl. Phys. 70 (1991) 3171
14. J. Wild, J. Macl, H. Sichova, P. Bohacek, J. Pracharova, Z. Janu, S. Civis and P. Kubat, Supercond. Sci. Technol. 11 (1998) 1341
15. S. Karimoto, S. Kubo, K. Tsuru and M. Suzuki, Jpn. J. Appl. Phys., 36 (1997) Pt. 1, No. 1A, 84
16. M. Yavuz, H. Maeda, L. Vance, H.K. Liu and S.X. Dou, Supercond. Sci. Technol. 11 (1998) 1166

17. P. Berberich, J. Tate, W. Dietsche, H. Kinder, Appl. Phys. Lett. 53, p. 925 (1989)
18. T. Terashima, K. Iijima, K. Yamamoto, Y. Bando, H. Mazaki, Jpn. J. Appl. Phys., 27, (1988) L91
19. J. Kwo, M. Hong, D.J. Trevor, R. M. Fleming, A.E. White, J.P. Mannaerts, R.C. Farrow, A.R. Kortan, K.T. Short, Physica C 162-164, (1989) 623
20. S. Prakash, K. Chou, G. Potwin, C.V. Deshpandey, H.J. Doerr, R.F. Bunshah, Supercond. Sci. Technol. 3, 543.
21. I. Bozovic, J.N. Eckstein, D.G. Schlom, J.S. Harris Jr. in Science and Technology of Thin Film Superconductors II, Eds. R. McConnell and S. Wolf, Plenum Press, New York, p. 267 (1990)
22. J.N. Eckstein, D.G. Schlom, E.S. Hellman, K.E. von Dessonneck, Z.J. Chen, C. Webb, F. Turner, J.S. Harris Jr., J. Vac. Sci. Technol. B7 (1989) 319
23. J.N. Eckstein, I. Bozovic, M.E. Klausmeier-Brown, G.F. Virshup, K.S. Ralls Thin Solid Films 216, (1992) 8.
24. M. Naito, Physica C 185-189 (1991) 1977
25. N.G. Chew, S.W. Goodyear, J.A. Edwards, J.S. Satchell, S.E. Blankinsop, R.G. Humphreys, Appl. Phys. Lett. 57 (1990) 2016
26. H. Sato, M. Naito, A. Tsukada, S. Karimoto and A. Matsuda, Physica C, 362 (2001) 186
27. S. Karimoto, S. Kubo, K. Tsuru, M. Suzuki, Jpn. J. of Appl. Phys. 36 (Part 1) (1997) 84
28. A. Marino, F. Ichikawa, H. Rodriguez and L. Linderer, Physica C, 282-287 (1997) 2277
29. C. Stolzel, M. Huth, H. Adrian, Physica C 204 (1992) 15
30. F. Breech, L. Cross, Applied Spectroscopy 16 (1962) 59
31. H.M. Smith, A.F. Turner, Applied Optics 4 (1965) 147

32. D. Dijkamp, T. Venkatesan, X.D. Wu, S.A. Shaheen, N. Jisrawi, Y.H. Min-Lee, W.L. McLean, M. Croft, Appl. Phys. Lett. 51 (1987) 619
33. D. B. Chrisey and G. K. Hubler, Eds, Pulsed Laser Deposition of Thin Films, John Wiley and Sons 1994
34. W.T. Lin and H.C. Hu, J. Crys. Growth 102 (1990) 354
35. M. M. Matthiesen, J.M. Graybeal, T.P. Orlando and J.B. Vander Sande, IEEE Trans. Magn., 27 (2) (1991) 1223
36. Y. Hakuraku and Z. Mori, J. of Appl. Phys., 73 (1), 1993, 309
37. P. Wagner, F. Hillmer, U. Frey, H. Adrian, T. Steinborn, L. Ranno, A. Elschner, I. Heyvaert and A. Bruynseraede, Physica C 215 (1993) 123
38. A. Ishii, T. Hatano, Physica C, 340 (2000) 173
39. L. Ranno, D. Martinez-Garcia and J. Perriere, Phys. Rev. B, Vol. 28, No. 18, (1993) 945
40. A. Cho, J. Vac. Sci. Tech., 8, (1971) S31-S38
41. S. K. Ghandhi, VLSI Fabrication Principles, John Wiley and Sons, New York, 1994
42. P. Sigmund, Physical Review 184 (1969) 383-416
43. M. Ohring, The Materials Science of Thin Films, Academic Press, Boston, 1992
44. S.H. Cohen and M.L. Lightbody, Eds, Atomic Force Microscopy/Scanning Tunneling Microscopy, Plenum Press, New York, 1997

APPENDIX A
CHARACTERIZATION TECHNIQUES

In order to investigate what the effects of various processing and deposition parameters have on the final film quality and properties, it is vital to characterize the film and the bulk materials. There exist a variety of techniques that are currently used, and are listed below.

a. Scanning electron microscopy and energy dispersive spectrometry
b. Transmission electron microscopy
c. Atomic force microscopy
d. X-ray diffraction

Each of these techniques will be described in some detail in the following pages.

A. SCANNING ELECTRON MICROSCOPY AND ENERGY DISPERSIVE SPECTROSCOPY

This technique is by far the most popular of techniques that is currently used in order to image the specimen at hand, and is also useful in getting a rough estimate of the composition of the sample. Scanning electron microscopes (SEMs) are modeled after optical microscopes, and yield similar information about the sample, namely the surface morphology, the shape and size of particles that may be present on the surface. This technique, however, is just a surface technique, and gives information only about the surface. The depth to which the analysis can be done depends on the operating parameters, and the specimen involved. A typical electron penetration depth would be about 5 micrometers. A beam of high-energy electrons is directed towards the sample using a conventional electron gun and the interaction of the electrons with the sample is studied.

In this technique, a narrow beam of coherent electrons, which are generated from a conventional electron gun are focused onto the sample of interest, and the interactions of the electron beam with the sample are studied using a varied array of detectors, which generates information about the sample. The SEM consists of a source of electrons, a focusing lens, scanning coils, a stage for mounting the sample, and an array of detectors.

A tungsten filament is resistively heated, which leads to the thermionic emission of electrons. A plate with a hole in it is placed a small distance in front of the cathode and is maintained at a positive potential with respect to the filament. This plate, the anode, attracts the electrons towards it. The hole in the plate allows electrons that are emitted at small enough angles with respect to the vertical axis of the gun to pass through. This arrangement ensures that the electrons seem to originate from a point source and have similar energies, and that the image information that is ultimately obtained is not erroneous.

The magnetic lens shown in figure 24 is an oversimplification, and consists of various parts. The first among these is a condenser lens. This is a magnetic lens that focuses the electrons into a parallel beam, and also eliminates high-angle electrons. The beam then travels through the condenser aperture, which eliminates more high angle electrons. The beam is then passed through a second condenser lens that forms it into a thin, tight, coherent beam. Then, a set of coils is used to scan the beam back and forth (hence the word “scanning” in the name) in a rastering fashion, in much the same fashion as a television picture. Finally, a focusing coil is used to adjust the focus of the beam. The beam is focused onto each point for a definite period of time before moving on to the next point. As an electron beam strikes the sample, it might interact with the sample, or not interact at all. The electrons that do not interact with the sample are of not much use. The electrons that interact are the ones of interest.

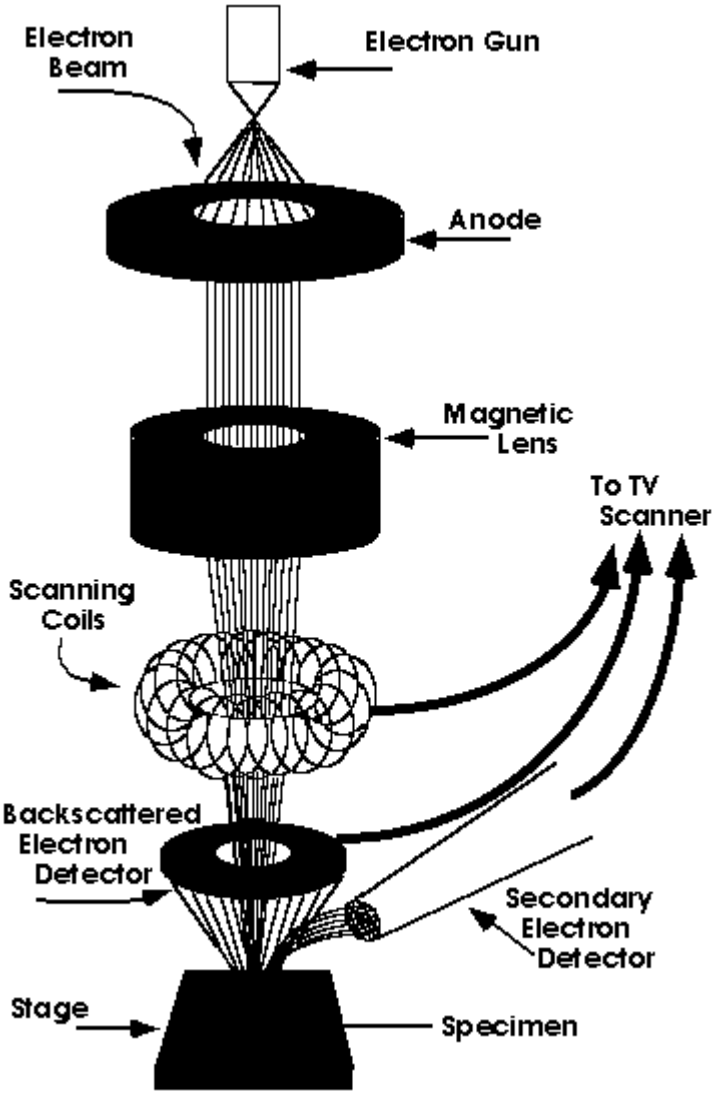

Figure 24. Schematic of a scanning electron microscope

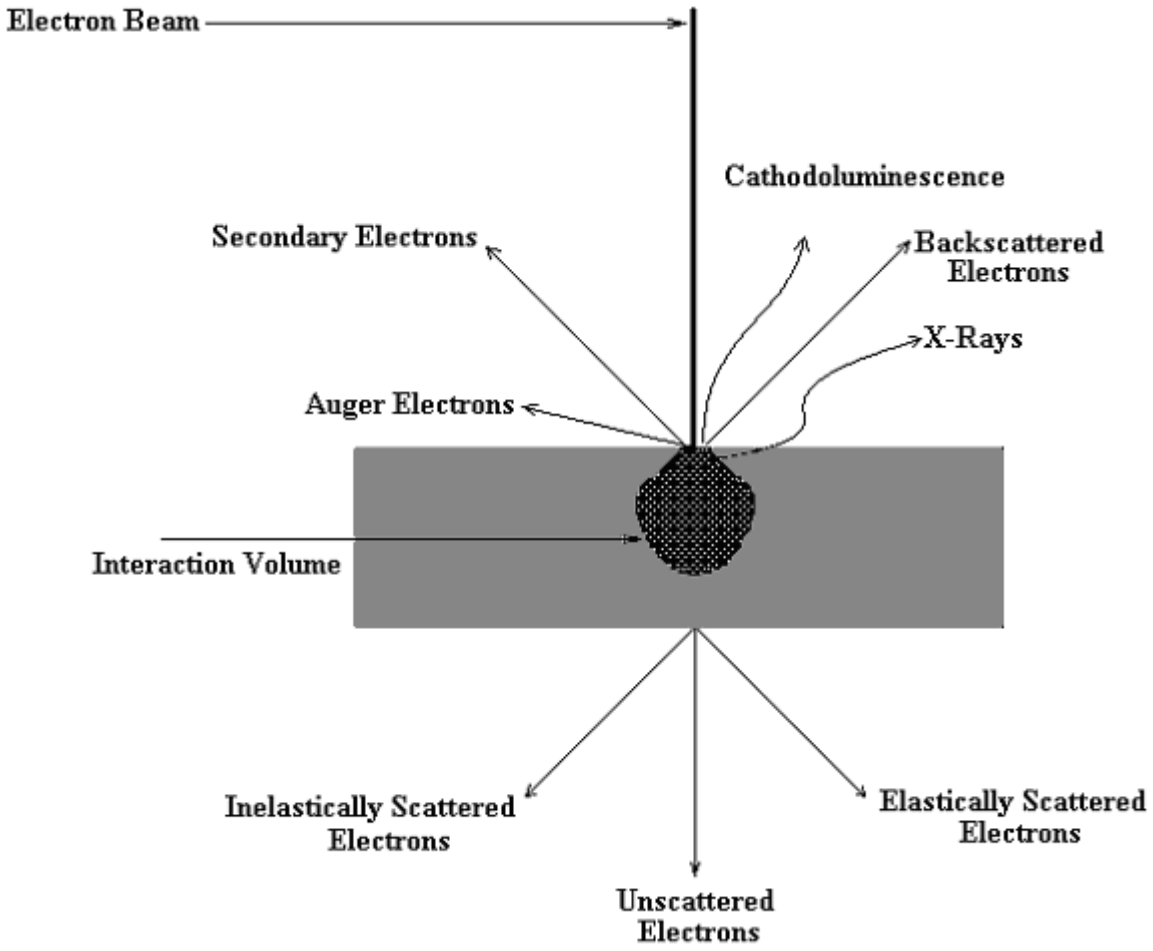

Figure 25. Interaction of electron beam with sample

Backscattered electrons are formed when an incident electron collides with an atom and is scattered by 180 degrees. The production of backscattered electrons varies directly with the specimen's atomic number. Elements with higher atomic numbers produce a larger backscatter yield, and hence appear brighter in a SEM micrograph.

Secondary electrons are produced when an electron from the electron beam passes near an atom and loses some of its energy to the latter. The energy imparted to the atom may cause it to lose a low energy electron, which is emitted as a secondary electron. Since these electrons have very low energy, of the order of 5 eV, the only secondary electrons that can exit the sample are those that are very close to the surface. Any changes in topography of the order of 10 nm will produce a change in the production of secondary electrons, and hence the topography of the surface can be mapped. The secondary electrons are collected using a "collector."

In the production of secondary electrons, the atom that interacts with the electron beam loses an electron. This vacancy can be filled by a higher energy electron, along with the emission of another low energy electron, which is emitted as an Auger electron. These Auger electrons have an energy that is characteristic of the element from which they were emitted.

After a secondary electron is produced, the energized atom loses some of its energy in returning to the ground state. This difference in energy is given off as an X-ray. The wavelengths of the X-rays emitted are also characteristic to the element from which they were emitted. A measure of the intensity and wavelength of the X-rays emitted will yield the compositional information of the specimen. This forms the basis of energy dispersive analysis of the specimen, which yields a semi-quantitative estimate of the elements present in the sample. Since the SEM uses an electron beam, the sample that is to be imaged needs to be conducting, at least at the surface. In order to image or analyze a non-

conducting sample, it has to be coated with some kind of conducting material. The most commonly used ones are either sputter deposited carbon or Au-Pd.

B. TRANSMISSION ELECTRON MICROSCOPY

The whole principle of transmission electron microscopy is based on the premise that the wavelength of light used for imaging puts a limit on the resolution. Optical microscopes use visible light, which has wavelengths ranging from 390-780 nm, depending on the color used.

Electrons were first discovered by J.J. Thomson in 1897, and their wave-like particles were discovered by Louis de-Broglie. The wavelength of an electron is given by the well-known de-Broglie relation,

$$\lambda = h/mv$$

where

λ = wavelength

h = Planck's Constant

m = Mass of the electron

v = velocity of the electron.

A typical electron accelerated by a voltage of 75 KV can have a theoretical wavelength less than 5 picometers. Unfortunately, this theoretical resolution cannot be attained, as the focusing lenses used in electron optics cannot be manipulated in the same was as glass lenses are. The lenses used in electron optics are similar to the primitive ones use by Leeuwenhoek when he made the first microscopes. This reduces the resolution that can be attained, but it is still better than optical microscopes.

The TEM is very similar to the SEM. The difference arises from the fact that in the SEM, the array of detectors is placed above the specimen; whereas in the

TEM, they are placed below the specimen. Further, electrons are not very efficient in penetrating a solid. Hence, the sample to be analyzed has to be exceedingly thin. The common preparation techniques used involve dimpling the sample, so that it has varying thickness. The sample is prepared by first dimpling it and then by ion milling to produce the hole inside. The hole ensures that some portions of the sample are thin enough to allow electrons to pass through. TEM can also be employed to obtain an electron diffraction pattern of samples. The samples that need to be analyzed may also be taken in the powder form.

C. ATOMIC FORCE MICROSCOPY

Atomic force microscopy is the extension of the more common stylus-profilometry to the atomic scale [44]. The basic principle is illustrated in figure 26. The AFM can be run in either of two modes: contact and non-contact. The contact mode is where the tip scans the sample in close contact with the surface and is the most commonly used mode. The force on the tip is repulsive with a mean value of 10^{-9} N. This force is set by pushing the cantilever against the sample surface with a piezoelectric positioning element. In contact mode AFM the deflection of the cantilever is sensed and compared in a DC feedback amplifier to some desired value of deflection. If the measured deflection is different from the desired value, the feedback amplifier applies a voltage to the piezo to raise or lower the sample relative to the cantilever to restore the desired value of deflection. The voltage that the feedback amplifier applies to the piezo is a measure of the height of features on the sample surface. It is displayed as a function of the lateral position of the sample. A few instruments operate in UHV but the majority operate in ambient atmosphere, or in liquids.

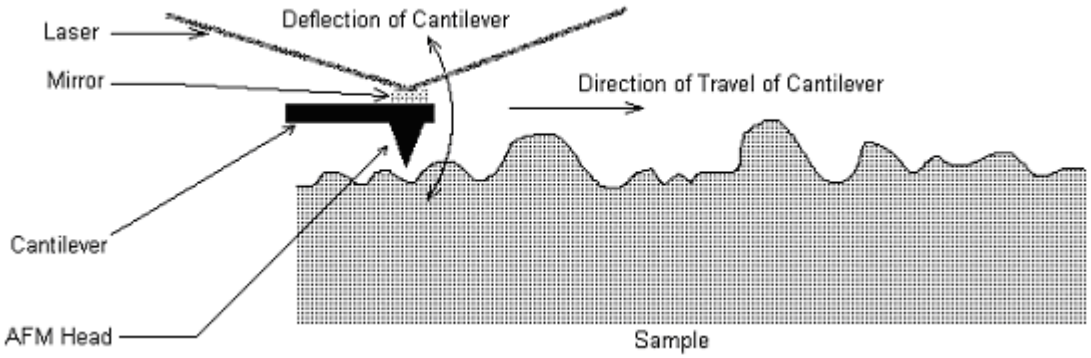

Figure 26. Principle of atomic force microscopy

Problems with the contact mode are caused by excessive tracking forces applied by the probe to the sample. The effects can be reduced by minimizing the tracking force of the probe on the sample, but there are practical limits to the magnitude of the force that can be controlled by the user during operation in ambient environments. A problem associated with this mode is that under ambient conditions, sample surfaces are covered by a layer of adsorbed gases consisting primarily of water vapor and nitrogen which is 10-30 monolayers thick. When the probe touches this contaminant layer, a meniscus forms and the cantilever is pulled by surface tension toward the sample surface. The magnitude of the force depends on the details of the probe geometry, but is typically on the order of 100 nanoNewtons. This meniscus force and other attractive forces may be neutralized by operating with the probe and part or the entire sample totally immersed in liquid. There are many advantages to operate AFM with the sample and cantilever immersed in a fluid. These advantages include the elimination of capillary forces, the reduction of Van der Waals' forces and the ability to study technologically or biologically important processes at liquid solid interfaces. However there are also some disadvantages involved in working in liquids. These range from nuisances such as leaks to more fundamental problems such as sample damage on hydrated and vulnerable biological samples. In addition, a large class of samples, including semiconductors and insulators, can trap electrostatic charge (partially dissipated and screened in liquid). This charge can contribute to additional substantial attractive forces between the probe and sample. All of these forces combine to define a minimum normal force that can be controllably applied by the probe to the sample. This normal force creates a substantial frictional force as the probe scans over the sample. In practice, it appears that these frictional forces are far more destructive than the normal force and can damage the sample, dull the cantilever probe and distort the resulting data. Also many samples such as

semiconductor wafers can not practically be immersed in liquid. An attempt to avoid these problem is the non-contact Mode.

A new era in imaging was opened when microscopists introduced a system for implementing the non-contact mode that is used in situations where tip contact might alter the sample in subtle ways. In this mode, the tip hovers 50 - 150 Å above the sample surface. Attractive Van der Waals forces acting between the tip and the sample are detected, and topographic images are constructed by scanning the tip above the surface. Unfortunately the attractive forces from the sample are substantially weaker than the forces used by contact mode. Therefore the tip must be given a small oscillation so that AC detection methods can be used to detect the small forces between the tip and the sample by measuring the change in amplitude, phase, or frequency of the oscillating cantilever in response to force gradients from the sample. For highest resolution, it is necessary to measure force gradients from Van der Waals forces that may extend only a nanometer from the sample surface. In general, the fluid contaminant layer is substantially thicker than the range of the Van der Waals force gradient and therefore, attempts to image the true surface with non-contact AFM fail as the oscillating probe becomes trapped in the fluid layer or hovers beyond the effective range of the forces it attempts to measure

Tapping mode is an important advance in AFM. This potent technique allows high resolution topographic imaging of sample surfaces that are easily damaged, loosely held to their substrate, or difficult to image by other AFM techniques. The tapping mode overcomes problems associated with friction, adhesion and electrostatic forces. Other difficulties that plague the conventional AFM scanning methods are overcome by alternately placing the tip in contact with the surface to provide high resolution and then lifting the tip off the surface to avoid dragging the tip across the surface. Tapping mode imaging is implemented in ambient conditions by oscillating the cantilever assembly at or near the cantilever's resonant frequency using a piezoelectric crystal. The piezo motion causes the

cantilever to oscillate with a high amplitude (typically greater than 20nm) when the tip is not in contact with the surface. The oscillating tip is then moved toward the surface until it begins to lightly touch, or tap the surface. During scanning, the vertically oscillating tip alternately contacts the surface and lifts off, generally at a frequency of 50,000 to 500,000 cycles per second. As the oscillating cantilever begins to intermittently contact the surface, the cantilever oscillation is necessarily reduced due to energy loss caused by the tip contacting the surface. The reduction in oscillation amplitude is used to identify and measure surface features.

During tapping mode operation, the cantilever oscillation amplitude is maintained constant by a feedback loop. Selection of the optimal oscillation frequency is software-assisted and the force on the sample is automatically set and maintained at the lowest possible level. When the tip passes over a bump in the surface, the cantilever has less room to oscillate and the amplitude of oscillation decreases. Conversely, when the tip passes over a depression, the cantilever has more room to oscillate and the amplitude increases (approaching the maximum free air amplitude). The oscillation amplitude of the tip is measured by the detector and input to the controller electronics. The digital feedback loop then adjusts the tip-sample separation to maintain a constant amplitude and force on the sample.

When the tip contacts the surface, the high frequency (50k - 500k Hz) makes the surfaces stiff (viscoelastic), and the tip-sample adhesion forces is greatly reduced. The tapping mode inherently prevents the tip from sticking to the surface and causing damage during scanning. Unlike contact and non-contact modes, when the tip contacts the surface, it has sufficient oscillation amplitude to overcome the tip-sample adhesion forces. In addition, the surface material is not pulled sideways by shear forces since the applied force is always vertical. Another advantage of the tapping mode technique is its large, linear operating

range. This makes the vertical feedback system highly stable, allowing routine reproducible sample measurements.

Tapping mode operation in fluid has the same advantages as in the air or vacuum. However, imaging in a fluid medium tends to damp the cantilever's normal resonant frequency. In this case, the entire fluid cell can be oscillated to drive the cantilever into oscillation. This is different from the tapping or non-contact operation in air or vacuum where the cantilever itself is oscillating. When an appropriate frequency is selected (usually in the range of 5,000 to 40,000 cycles per second), the amplitude of the cantilever will decrease when the tip begins to tap the sample, similar to the tapping mode operation in air. Alternatively, very soft cantilevers can be used to get good results in fluids. The spring constant is typically 0.1 N/m compared to the tapping mode in air where the cantilever may be in the range of 1-100 N/m.

D. X-RAY DIFFRACTION

X-ray diffraction is one of the most important methods of determining the structure of any sample, powder or single crystal. The essence of X-ray diffraction is the well-known Bragg's Law. The Bragg condition for constructive interference is

$$m\lambda=2d\mathrm{Sin}\theta$$

The atoms in a certain plane of the crystal lattice collectively behave like mirrors, and hence the principles of optics can be used to determine the angles at which constructive interference occurs. In practice, X-rays of a known wavelength are directed towards the sample to be analyzed. The sample is then rotated, thereby changing the angle of incidence θ. A detector is placed on the other side of the sample, which detects the intensity of the reflected x-rays, thereby detecting the presence or absence of a peak. A graph of 2θ vs. Intensity of the X-ray beam is then plotted. This is compared to a standard reference and the crystal structure of the sample in question can be determined.

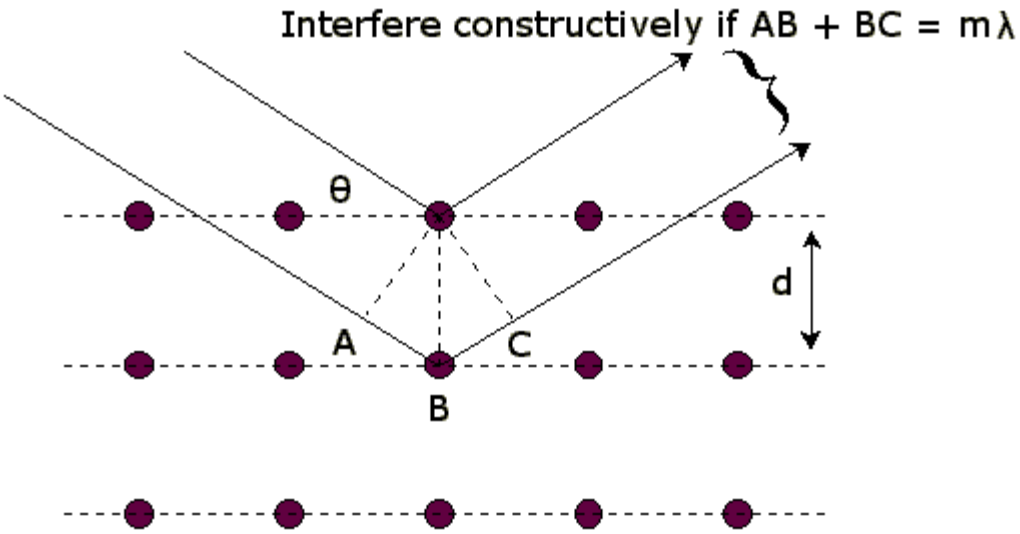

Figure 27. Principle of X-ray diffraction

VITA

Santhana Gopinath Ganapathy Subramanian was born in Bombay, India on October 21, 1978. He graduated from the Frank Anthony public school in Bangalore, India in 1994. He received his B.E. in mechanical engineering from the University of Mysore in 2000. He intends to pursue a PhD in mechanical engineering at Texas A&M University. He can be reached at the following address:

"Gananath", No. 25, Fourth Cross,
Jaibharath Nagar,
Bangalore 560 033
INDIA